Synthesis, Physicochemical and Biochemical Studies of 1′,2′-Oxetane Constrained Adenosine and Guanosine Modified Oligonucleotides, and Their Comparison with Those of the Corresponding Cytidine and Thymidine Analogues

Pushpangadan I. Pradeepkumar,[†] Pradeep Cheruku,[†] Oleksandr Plashkevych,[†] Parag Acharya,[†] Suresh Gohil,[‡] and Jyoti Chattopadhyaya*,[†]

Contribution from the Department of Bioorganic Chemistry, Box 581, Biomedical Center, University of Uppsala, S-75123, Uppsala, Sweden, and Department of Chemistry, Swedish University of Agricultural Sciences, Box 7015, Uppsala, Sweden

Received March 19, 2004; E-mail: jyoti@boc.uu.se

Abstract: We have earlier reported the synthesis and antisense properties of the conformationally constrained oxetane-**C** and **-T** containing oligonucleotides, which have shown effective down-regulation of the proto-oncogene c-myb mRNA in the K562 human leukemia cells. Here we report on the straightforward syntheses of the oxetane-**A** and oxetane-**G** nucleosides as well as their incorporations into antisense oligonucleotides (AONs), and compare their structural and antisense properties with those of the **T** and **C** modified AONs (including the thermostability and RNase H recruitment capability of the AON/RNA hybrid duplex by Michaelis–Menten kinetic analyses, their resistance in the human serum, as well as in the presence of exo and endonucleases).

Introduction

Antisense oligonucleotides (AONs), based on elegant principle of Watson–Crick base pairing with the complementary mRNA, have been shown to be capable of down-regulation of the genes of interest.[1] AONs are being developed as a gene knock-off tool in functional genomics as well as therapeutic agent[1], since their first inception in 1978.[2] In the clinical perspective, the antisense technology utilizing AONs, which elicit the RNase H cleavage of target RNA for the down-regulation of the disease causing genes (Figure 1), offers advantages in terms of efficiency and dosage compared to those AONs, which offer gene silencing by the steric blockage of the ribosomal read-through.[3] The RNase H cleavage efficiency of the AON/RNA hybrid duplex can be best exploited for potential therapeutic usage when the AONs show the adequate nuclease resistance in vivo, sequence specificity, cell deliverability, nontoxicity, and favorable pharmacokinetics.[1,4] Chemical modifications are warranted to achieve those goals, however, in most of the cases the nature of modifications hampers one or more of the above-mentioned requirements.[4] Since the widely studied phosphorothioate AONs are marred with their low sequence specificity and higher (1–3 orders of magnitude) binding affinity
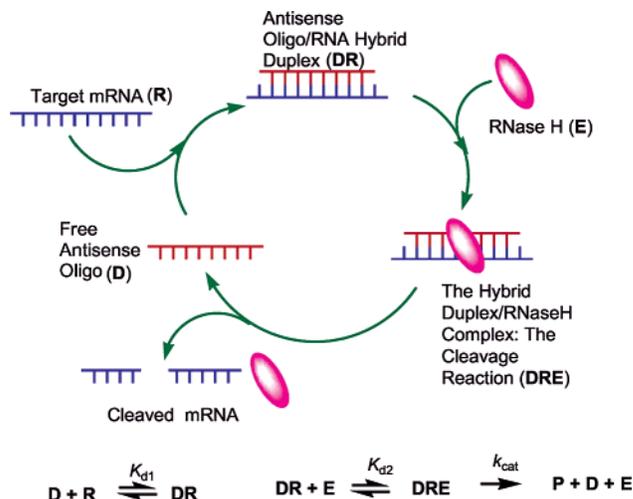

Figure 1. Catalytic RNase H promoted cleavage of the target mRNA through the formation of antisense Oligonucleotide/RNA Hybrid Duplex. The kinetic scheme of the RNase H hydrolysis is shown in the bottom part of the cartoon, where **D** is AON (antisense Oligo); **R** is the target RNA; K_{d1} is the equilibrium constant of dissociation of the heteroduplex **DR** and K_{d2} is equilibrium constant of dissociation of the substrate–enzyme complex **DRE**.

for various cellular proteins, especially the heparin binding proteins, which accounts for many of their reported nonantisense effects,[5] the search for alternative chemical routes of nucleoside modification without changing the phosphodiester backbone has been intensified in the past decade.

[†] University of Uppsala, http://www.boc.uu.se.
[‡] Swedish University of Agricultural Sciences.

(1) (a) Scherer, L. J.; Rossi, J. J. *Nat. Biotech.* **2003**, *21*, 1457. (b) Dias, N.; Stein, C. A. *Mol. Cancer. Ther.* **2002**, *1*, 347. (c) Opalinska, J. B.; Gewirtz, A. M. *Nat. Rev. Drug. Discov.* **2002**, *1*, 5303. (d) Agrawal, S.; Kandimalla, E. R. *Mol. Med. Today* **2000**, *6*, 72.
(2) Zamecnik, P.; Stephenson, M. L. *Proc. Natl. Acad. Sci. U.S.A.* **1978**, *75*, 280.
(3) Zamaratski, E.; Pradeepkumar, P. I.; Chattopadhyaya, J. *J. Biochem. Biophys. Methods* **2001**, *48*, 189.
(4) Kurreck, J. *Eur. J. Biochem.* **2003**, *270*, 1628.

(5) (a) Stein, C. A. *J. Clin. Invest.* **2001**, *108*, 641. (b) Lebedeva, I.; Stein C. A. *Annu. Rev. Pharmacol.* **2001**, *41*, 403. (c) Levin, A. A. *Biochim. Biophys. Acta* **1999**, *1489*, 69.

In recent times, AONs incorporated with sugar modified nucleosides have been widely pursued as a valuable alternative.[6,7,17] Among these, the AONs modified with *North*-conformationally ($-1° < P < 34°$)[8] constrained nucleotides have attracted much attention because of their ability to drive the AON strand of the AON/RNA hybrid duplex to the RNA/RNA type, thereby increasing the target affinity.[6,7] They can be broadly classified into three groups. The first group comprises of AONs incorporated with various 2′-*O*-alkyl moieties [$-CH_3$,[9] $-CH_2-CH_2-O-CH_3$,[9] $-CH_2-CH_2-CH_2-NH_2$[7,10] etc.] or electron withdrawing functional groups such as the F[11] in the *ribo* configuration. The monomer units of 2-*O*-alkyl modified compounds exist in solution in the *North-South* pseudorotational equilibrium (with very little preference for the *North*-type sugars[12]), however, upon incorporation into the AON and subsequent hybridization with the target RNA, they impart 3′-*endo* conformation to their sugar moiety and to the neighboring nucleotides in a varying extent.[13] The second group of AONs encompasses nucleic acids containing pyranose derivatives such as the hexitol nucleic acids[14] and their AON/RNA hybrid duplexes mimic RNA/RNA type helix.[6,14] The third group of AONs consists of those containing conformationally constrained bicyclic or tricyclic monomer nucleotide units.[15] Because of their conformational preorganization at the monomer level itself, the complete or sometimes partial modification of the AON strand with *North*-conformationally constrained units[16] drive the AON/RNA duplex to the rigid RNA/RNA type duplex[17] which results in the loss of the RNase H cleavage efficiency.[3] However, RNase H eliciting capability can partly or fully be regained by adopting various mixmer and gapmer strategies utilizing these modifications.[18,19] In some cases such as in the β-D-LNA

modified AONs, a gap size of $8-10$ nucleotides was necessary to recruit the effective RNase H cleavage capability of the target RNA.[19,20] It is likely that use of such a lengthy unmodified phosphodiester oligonucleotide gaps could be harmful in view of the endonuclease susceptibility of the AONs.[21]

We have developed novel 1′,2′-oxetane locked nucleosides, [1-(1′,3′-*O*-anhydro-β-D-psicofuranosyl) nucleosides] which have a unique fixed *North-East* sugar conformation,[22−24] and belong to the third class of the above-mentioned conformationally constrained nucleosides. Even though the T_m of the AON/RNA hybrid drops by ∼$5−6$ °C/oxetane-thymidine (***T***) modification, the mixmer AON/RNA hybrids incorporated with ***T*** units were found to be substrates for RNase H promoted cleavage as good as the native hybrid.[22−24] However, the incorporation of the oxetane-cytidine (***C***) moiety into the AONs imparts only ∼3 °C loss in T_m per oxetane-modification.[24] The loss of the thermodynamic stability in case of oxetane-***T*** and -***C*** was fully or partly regained by the introduction of the nontoxic[25,26] DPPZ (dipyridophenazine) group[25] at the 3′ end, and it gave additional stability against exonucleases similar to that of the phosphorothioate AONs.[22c,24] Another interesting observation was that only 4 deoxynucleotide gaps in the AON strand were needed to achieve the RNase H cleavage of the RNA in their hybrids duplexes.[22,24] Michaelis−Menten kinetics of the RNase H cleavage showed that V_{max} and K_m increase with increase in the number (one to three) of ***T***/***C*** modifications in the AONs, indicating higher catalytic activity and lower enzyme binding affinity of the oxetane-modified AON/RNA hybrids.[23,24] The endonuclease cleavage of these molecules was reduced significantly and it was proportional to the number of the oxetane modified nucleotides per AON molecule: single modification gave 2-fold protection to the cleavage and double and triple modification gave 4-fold protection compared to that of the native phosphodiester oligonucleotide.[22c,24]

The antisense oligo constructs with the oxetane-***C*** and 3′-DPPZ were found to be nontoxic in K562 human leukemia cells and have been successfully employed to down-regulate the proto-oncogene c-myb in a very efficient manner.[26] The QRT-PCR and Western blotting (the "gold standard" in antisense

(6) Herdewijn, P. *Biochim. Biophys. Acta* **1999**, *1489*, 167.
(7) Manoharan, M. *Biochim. Biophys. Acta* **1999**, *1489*, 117.
(8) de Leeuw, H. P. M.; Haasnoot, C. A. G.; Altona, C. *Isr. J. Chem.* **1980**, *20*, 108.
(9) Martin, P. *Helv. Chim. Acta* **1995**, *78*, 486.
(10) Griffey, R. H.; Monia, B. P.; Cummins, L. L.; Frier, S. M.; Greig, M. J.; Guinosso, C. J.; Lesnik, E.; Manalili, S. M.; Mohan, V.; Owens, S.; Ross, B. R.; Sasmor, H.; Wancewicz, E.; Wieler, K.; Wheeler, P. D.; Cook, P. D. *J. Med. Chem.* **1996**, *39*, 5100.
(11) Kawasaki, A. M.; Casper, M. D.; Frier, S. M.; Lesnik, E. A.; Zounes, M. C.; Cummins, L. L.; Gonzalez, C.; Cook, P. D. *J. Med. Chem.* **1993**, *36*, 831.
(12) Kawai, G.; Yamamoto, Y.; Amimura, T.; Masegi, T.; Sekine, M.; Hata, T.; Iimori, T.; Watanabe, T.; Miyazawa, T.; Yokoyama, S. *Biochemistry* **1992**, *31*, 1040.
(13) Nishizaki, T.; Iwai, S.; Nakamura, H. *Biochemistry* **1997**, *36*, 2577.
(14) Hendrix, C.; Rosenmeyer, H.; Bouvere, B. D.; Aerschot, A. V.; Seela, F.; Herdewijn, P. *Chem. Eur. J.* **1997**, *3*, 1513.
(15) (a) Kvaerno, L.; Wengel, J. *Chem. Commun.* **2001**, *16*, 1419. (b) Leumann, C. *Bioorg. Med. Chem.* **2002**, *10*, 841. (c) Meldgaard, M.; Wengel, J. *J. Chem. Soc., Perkin Trans. 1* **2000**, 3539.
(16) (a) Tarkoy, M.; Bolli, M.; Schweizer, B.; Leumann, C. *Helv. Chim. Acta* **1993**, *76*, 481. (b) Altman, K.-H.; Kesselring, R.; Francotte, E.; Rihs, G. *Tetrahedron Lett.* **1994**, *35*, 2331.(c) Siddiqui, M. A.; Ford, H.; George, C.; Marquez, V. E. *Nucleosides Nucleotides* **1996**, *15*, 235 (d) Marquez, V. E.; Siddiqui, M. A.; Ezzitouni, A.; Russ, P.; Wang, J.; Wanger, W. R.; Matteucci, D. M. *J. Med. Chem.* **1996**, *39*, 3739. (e) Obika S.; Nanbu D., Hari Y., Morio, K.; In, Y.; Ishida, T.; Imanishi, T. *Tetrahedron Lett.* **1997**, *38*, 8735. (f) Koshkin, A. A.; Singh, S. K.; Nielson, P.; Rajwanshi, V. K.; Kumar R.; Meldgaard, M.; Wengel, J. *Tetrahedron* **1998**, *54*, 3607. (g) Wang, G.; Giradet, J.-L.; Gunic, E. *Tetrahedron* **1999**, *55*, 7707. (h).Wengel, J. *Acc. Chem. Res.* **1999**, *32*, 301. (i) Sekine M, Kurasawa O.; Shohda K.; Seio K.; Wada.; T. *J. Org. Chem.* **2000**, *12*, 3571. (j) Morita, K.; Hasegawa, C.; Kaneko, M.; Tsutsumi, S.; Sone, J.; Ishikawa, T.; Imanishi, T.; Koizumi, M. *Bioorg. Med. Chem. Lett.* **2002**, *12*, 73. (k) Imanishi, T.; Obika, S. *Chem. Commun.* **2002**, *16*, 1653. (l) Wang, G. *Tetrahedron Lett.* **1999**, *40*, 6343. (m) Sugimoto, I.; Shuto, S.; Mori, S.; Shigeta, S.; Matsuda, A. *Tetrahedron Lett.* **1999**, *9*, 385. (n) Steffens, R.; Leumann, C. *Helv. Chim. Acta* **1997**, *80*, 2426. (o) Nielsen, P.; Petersen, M.; Jacobsen, J. P *J. Chem. Soc., Perkin Trans. 1* **2000**, 3706. (p) Christiensen, N. K.; Andersen, A. K. L.; Schultz, T. R.; Nielsen, P. *Org. Biomol. Chem.* **2003**, *1*, 3738. (q) Wengel, J.; Peterson, M. *Trends Biotechnol.* **2003**, *21*, 74. (r) Kvaerno, L.; Wengel, J. *J. Org. Chem.* **2001**, *66*, 12, 5498.
(17) Acharya, P.; Cheruku, P.; Chatterjee, S.; Acharya, S.; Chattopadhyaya, J. *J. Am. Chem. Soc.* **2004**, *126*, 2862.

(18) Lima, W. F.; Crooke, S. T. *Biochemistry* **1997**, *36*, 390.
(19) (a) Kurreck, J.; Wyszko, E.; Gillen, C.; Erdmann, V. A. *Nucleic Acids Res.* **2002**, *30*, 1911. (b) Braasch, A. D.; Liu, Y.; Corey, D. R. *Nucleic Acids Res.* **2002**, *30*, 5160.
(20) Frieden, M.; Christensen, S. M.; Mikkelsen, N. D.; Rosenbohm, C.; Thrue, C. A.; Westergaard, M.; Hansen, H. F.; Orum, H.; Koch, T. *Nucleic Acids Res.* **2003**, *31*, 6325.
(21) (a) Sands, H.; Gorey-Feret, L. J.; Ho, S. P.; Bao, Y.; Cocuzza, A. J.; Chidester, D.; Hobbs, F. W. *Mol. Pharmacol.* **1995**, *47*, 636. (b) Miyao, T.; Takakura, Y.; Akiyama, T.; Yoneda, F.; Sezaki, H.; Hashida, M. *Antisense Res Dev.* **1995**, *5*, 115. (c) Uhlmann, E.; Peyman, A.; Ryte, A.; Schmidt, A.; Buddecke, E. *Methods Enzymol.* **2000**, *313*, 268. (d) Peyman, A.; Helsberg, M.; Kretzschmar, G.; Mag, M.; Ryte, A.; Uhlmann, E. *Antiviral Res.* **1997**, *33*, 135.
(22) (a) Pradeepkumar, P. I; Zamaratski. E.; Foldesi A.; Chattopadhyaya J. *Tetrahedron Lett.* **2000**, *41*, 8601. (b) Pradeepkumar, P. I.; Zamaratski E.; Foldesi A.; Chattopadhyaya J. *J. Chem. Soc., Perkin Trans. 2* **2001**, 402. (c) Pradeepkumar, P. I.; Chattopadhyaya J. *J. Chem. Soc., Perkin Trans. 2* **2001**, 2074. (d) Boon, E. M.; Barton, J. K.; Pradeepkumar, P. I.; Isaksson, J.; Petit, C.; Chattopadhyaya, J. *Angew. Chem., Int. Ed.* **2002**, *41*, 3402.
(23) Amirkhanov, N. V.; Pradeepkumar, P. I.; Chattopadhyaya, J. *J. Chem. Soc., Perkin Trans. 2* **2002**, 976.
(24) Pradeepkumar, P. I.; Amirkhanov, N. V.; Chattopadhyaya, J. *Org. Biomol. Chem.* **2003**, *1*, 81.
(25) (a) Ossipov, D.; Zamaratski, E.; Chattopadhyaya, J. *Helv. Chim. Acta* **1999**, *82*, 2186. (b) Zamaratski, E.; Ossipov, D.; Pradeepkumar, P. I.; Amirkhanov, N. V.; Chattopadhyaya, J. *Tetrahedron* **2001**, *57*, 593.
(26) Opalinska,J. B.; Kalota, A.; Rodriquez, L.; Henningson, H.; Gifford, L. K.; Lu, P.; Jen, K.-Y.; Paradeepkumar, P. I.; Barman, J.; Kim, T. K.; Swider, C.; Chattopadhyaya, J.; Gewirtz, A. M. *Proc. Natl. Acad. Sci. U.S.A.* **2004**, under review.

|			
Native 20mer (PO)	AON (**1**)	3'-d(T T A C G T A C A G T G T C C G C C C T)-5'	$T_m = 74\ ^\circ C, \Delta T_m = 0\ ^\circ C$
20-3**A**	AON (**2**)	3'-d(T T **A** C G T A**C** A**G** T G T C C G C C C T)-5'	$T_m = 73\ ^\circ C, \Delta T_m = -1\ ^\circ C$
20-3**G**	AON (**3**)	3'-d(T T A C **G** T A C A **G** T G T C C **G** C C C T)-5'	$T_m = 74\ ^\circ C, \Delta T_m = 0\ ^\circ C$
20-3**C**	AON (**4**)	3'-d(T T A **C** G T A **C** A G T G T C **C** G C C C T)-5'	$T_m = 61\ ^\circ C, \Delta T_m = -13\ ^\circ C$
20-2**A** + **G**	AON (**5**)	3'-d(T T **A** C G T A C **A** G T G T C C **G** C C C T)-5'	$T_m = 73\ ^\circ C, \Delta T_m = -1\ ^\circ C$
20-2**G** + **A**	AON (**6**)	3'-d(T T A C **G** T A C **A** G T G T C C **G** C C C T)-5'	$T_m = 73\ ^\circ C, \Delta T_m = -1\ ^\circ C$
20-3**A** + 3**G**	AON (**7**)	3'-d(T T **A** C **G** T A **C** A **G** T **G** T C C **G** C C C T)-5'	$T_m = 74\ ^\circ C, \Delta T_m = 0\ ^\circ C$
20-3**A** +DPPZ	AON (**8**)	**DPPZ**-p-3'-d(T T **A** C G T **A**C **A** G T G T C C G C C C T)-5'	$T_m = 75\ ^\circ C, \Delta T_m = +1\ ^\circ C$
20-3**G** + DPPZ	AON (**9**)	**DPPZ**-p-3'-d(T T A C **G** T A C A **G** T G T C C **G** C C C T)-5'	$T_m = 76\ ^\circ C, \Delta T_m = +2\ ^\circ C$
20-3**T**	AON (**10**)	3'-d(T T A C G **T** A C A G **T** G **T** C C G C C C T)-5'	$T_m = 59\ ^\circ C, \Delta T_m = -15\ ^\circ C$
Native 20mer (PS)	AON (**11**)	3'-d(T T A C G T A C A G T G T C C G C C C T)-5'	
20-3'-**C** modified	AON (**12**)	3'-d(**C A G** C G T A C A G T G T C C G C C **C T**)-5'	
Target 20mer RNA	RNA (**13**)	5'-r(A A U G C A U G U C A C A G G C G G G A)-3'	
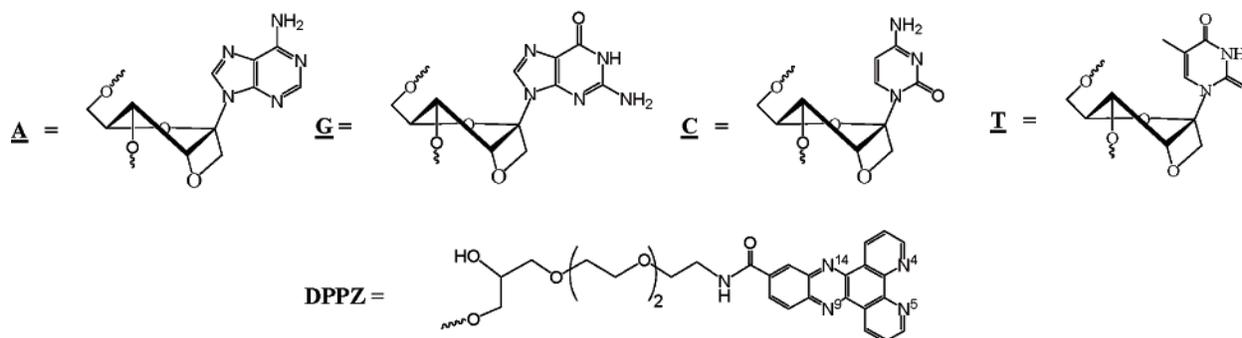
Figure 2. Sequences and T_ms of various heteroduplexes containing oxetane-modified AONs and their target RNA. The T_m and the differences in T_m (ΔT_m) with respect to that of the native phosphodiester AON (**1**) for 20mer AONs are also shown for comparison.

efficacy[5a]) have shown that rationally designed oxetane-*C* modified AONs were highly efficient both in diminishing the c-myb mRNA (85% has been reduced) and the c-myb protein (70% of its expression was found to be halted) of the targeted gene. On the basis of the amount of AON uptake after delivery, determined by slot blot, it was apparent that the oxetane modified AONs are 5−6 times more efficient antisense agents than those of the corresponding isosequential phosphorothioate analogue.[26]

The above-mentioned successful antisense design combining the oxetane-*C* units and 3′-DPPZ group prompted us to investigate the properties of the oxetane-purine modified AONs. Here, we report the synthesis of the oxetane-*A* [9-(1′,3′-*O*-anhydro-β-D-psicofuranosyl)adenine] and the oxetane-*G* [9-(1′,3′-*O*-anhydro-β-D-psicofuranosyl)guanine] units (Figure 2) as well as the structure, target affinity, RNase H cleavage, exo and endonuclease tolerance of AONs (**2**−**9**) incorporating these units. Michaelis−Menten kinetics of *E. coli* RNase H1 promoted cleavage has been carried out for the oxetane-*A* and -*G* modified AONs (**2** and **3**)/RNA (**13**) hybrids, and the kinetic parameters are compared with those of the oxetane-*C* modified (**4**) and native AON (**1**)/RNA (**13**) hybrids.

Results and Discussions

(A) Binding Affinity of the Oxetane-*A* and -*G* Modified AONs to the Target RNA and the Thermodynamic Properties of the Modified AON/RNA Hybrids. When tested for target affinity, the triple oxetane-*A* modified AON (**2**)/RNA (**13**) and the triple oxetane-*G* modified AON (**3**)/RNA (**13**) have

exhibited melting temperatures very similar to that of the native AON (**1**)/RNA (**13**) hybrid duplex (Figure 2). However, the introduction of the triple *C* modifications as in AON (**4**)/RNA (**13**) causes 4 °C drop in T_m per oxetane-modification while the introduction of the oxetane-*T* modifications into the AON (**10**)/RNA (**13**) hybrid makes it even more unstable showing a T_m drop of 5 °C per oxetane-*T* modification (Figure 2). This clearly shows that the oxetane−pyrimidine units have considerable destabilizing effect on the thermostability of the AON/ RNA hybrids compared to those of their purine counterparts. The mixed sequences of the oxetane-*A* and -*G* moieties, such as AONs (**5**−**7**), have also shown similar target binding affinities close to that of the native AON (**1**) (Figure 2). It should be noted that T_m enhancement effect of the 3′-DPPZ group which we have observed earlier in the studies of 9mer and 15mer AON/ RNA hybrids[22c,24] has been considerably reduced in the case of 20mer AON/RNA hybrids studied here.

To shed more light on the differential binding affinities of the oxetane modified AONs to the target RNA (**13**), we have elucidated thermodynamic parameters (Table 1), based on the concentration dependent T_m analysis of the native AON (**1**)/ RNA (**13**) duplex and those of the triple oxetane-purine (**2** and **3**) or pyrimidine-modified AONs (**4** and **10**). It has emerged that the thermodynamic parameters of the triple oxetane-*G* modified AON (**3**)/RNA (**13**) duplex are very close to that of the native AON (**1**)/RNA (**13**) duplex. However, ΔH° and ΔS° of the triple oxetane-*A* modified AON (**2**)/RNA (**13**) duplex are slightly lower (5.5 kJ/mol drop in ΔG°) than those of the

Table 1. Thermodynamic Parameters of 20Mer AON (**1**−**4** and 10)/RNA (**13**) Hybrids Determined from T_m^{-1} vs $\ln(C_T/4)$ Plots

AONs	T_m (°C)	$-\Delta H°$ (kJ/mol)	$-\Delta S°$ (J/K·mol)	$-T\Delta S°$	$-\Delta G°$ (298 K) (kJ/mol)	$\Delta\Delta G°$ (kJ/mol)
native 20mer (**1**)	74	740.4 ± 22.3	2016 ± 64	600.9	139.5	
20−3**A** (**2**)	73	714.2 ± 22.5	1946 ± 65	580.2	134.0	−5.5
20−3**G** (**3**)	74	747.7 ± 13.9	2034 ± 40	606.4	141.3	+1.8
20−3**C** (**4**)	61	661.5 ± 13.5	1860 ± 40	554.5	107.0	−32.5
20−3**T** (**10**)	59	646.6 ± 20.5	1853 ± 62	544.5	102.3	−37.2

native duplex and the triple oxetane-**G** modified hybrid duplexes. The triple oxetane-**C** modified AON (**4**)/RNA (**13**) as well as the triple oxetane-**T** modified AON (**10**)/RNA (**13**) duplex have shown large enthalpic destabilization and slight entropic stabilization, which resulted in the net loss of 32.5 kJ/mol in $\Delta G°$ for the triple **C** and 37.2 kJ/mol net loss for the triple **T** modified hybrids compared to that of the native duplex. Apparently, the large drop in enthalpy of the oxetane-modified pyrimidine AON/RNA duplexes contributes to the destabilization of the duplex which reflects in the weakening of the stacking and hydrogen bonding interactions. But it is not clear which force is dominantly disturbed during the duplex formation. The nucleic acid mediated charge transport measured by chronocoulometry[22d] has revealed that the stacking/dynamics perturbations owing to the incorporation of the oxetane-**T** unit in a DNA/RNA duplex are similar to those of the native hybrid duplex,[22d] while the complete charge attenuation was observed for the oxetane-**T** incorporated DNA/DNA homoduplex. However, this better accommodative nature of *North-East* constrained oxetane-**T** unit in the DNA/RNA duplexes is not reflected in its thermostability which is somewhat poorer (T_m drop of 6 °C/modification) than that of the native duplex. Two probable reasons for the weakening of thermostability could be (i) perturbation of the intrastrand stacking because of the *North*-type sugar among the neighboring *South*-type sugars along the DNA strand, or (ii) a possible steric clash between the oxetane ring and the hydrogen-bonding center of the aglycon, which is more pronounced in the pyrimidines than in purines (for example the distance between C1′ to H-bonding center N^{3}H is 4.9 Å in oxetane-**T** while the distance between C1′ to H-bonding center N^1 in oxetane-**A** is 5.4 Å). Clearly, more studies are needed, some of which are under way in our laboratory, to elucidate the reasons dictating the stability of the oxetane-modified AON/RNA hybrids.

(B) CD Spectra of the Oxetane-Modified AON/RNA Hybrids. Since circular dichroism (CD) spectroscopy is an effective tool to measure the global helical conformation of nucleic acids, we have recorded CD spectra of the oxetane-modified AON/RNA hybrids (Figure S1 in Supporting Information). Similar to the results obtained in our previous studies[22] with the oxetane-**T** modified 15mer AON/RNA hybrids, it was found that the introduction of the oxetane-**A** and oxetane-**G** units into the 20mer AONs (**2** and **3**) has not altered the global conformation of the duplexes compared to that of the native AON (**1**)/RNA (**13**) duplex (Figure S1 in Supporting Information). From these results, it is evident that CD has failed to detect the *local conformational changes* brought by the oxetane modification(s), which has in fact been sensed by RNase H as it can be seen from its cleavage pattern (vide infra).

(C) Endonuclease, Exonuclease, and Human Serum Stability of Oxetane-Modified AONs. When treated with the endonuclease (DNase 1), the triple oxetane-**A** (**2**) and triple

oxetane-**G** (**3**) modified AONs offered no resistance toward the cleavage by the enzyme (Figure 3, Figure S2 in Supporting Information). The half-life of the AON (**7**) with the three **A** and three **G** units was found to be about 2 h, which is about half of that observed for the triple oxetane-**C** modified AON (**4**) studied under similar conditions. These results reveal the high susceptibility of the oxetane-purine modified AONs toward the DNase 1 promoted cleavage.

To date, only very limited information is available for the structural and cleavage characteristics of DNase 1 with single stranded AONs. Although the DNase 1 cleavage has limited sequence specificity,[27] the crystal structure of the DNase 1 with various short oligonucleotide duplexes,[28] has revealed that in addition to the minor groove width and DNA flexibility, the *local sequence preference* is crucial for the proper alignment of the phosphodiester bond for the cleavage reaction. It has emerged that three nucleotides toward the 5′- and 3′-end of the cleavage site have significant influence on the cleavage properties. On the basis of the cleavage characteristics of various DNA duplexes, Herrera and Chaires[29] found that among those 6 nucleotides around the cleavage site, the nucleotide sequences at position 3 (denoted as −3) and 2 (denoted as −2) toward the 5′-end (Figure 3) and nucleotide at position 2 (denoted as +2) toward the 3′-end of the cleavage site are very crucial in determining the major cleavage sites and cleavage rates of DNA duplexes by DNase 1.[29] This is because the NH$_2$ of G at position −3 cause steric clash with arginine 41 of the enzyme and hamper the cleavage rate.[27,29] Tyrosine-76 has shown favorable interactions with T/C moieties at the position −2. At the position +2 toward 3′-end presence of T is highly disfavored.[28,29]

Our results can be partly explained based on the *local sequence* requirements described above. In the native AON (**1**), the cleavage sites have been restricted to the 5′-end of the oligo and the major cleavage site was found to be at G9, which is in accordance with the aforementioned general requirements (Figure 3, Figure S2 in Supporting Information). In all of the oxetane-modified AONs, the major and minor cleavage sites were observed at one or two nucleotides away from the modified sites. This clearly shows that the oxetane ring in the nucleotides interferes with the catalytic core of the enzyme and prevents the cleavage. Also, the modified residues might alter the flexibility and the geometrical requirements of phosphate required for the cleavage. In the triple **A** modified AON (**2**) all the cleavage sites of the native AON (**1**) are retained because there is no oxetane modification present at those cleavage sites. This explains why the extent of cleavage in the triple **A** modified AON (**2**) is very similar to that of the native AON (**1**). In the triple G modified AON (**3**) the major cleavage site has been shifted to the T8 instead of G9, which is probably because of the presence of the oxetane-**G** at G11 position (Figure 3, Figure S2 in Supporting Information). But the oxetane-**G** at +3 did not affect the cleavage rate. Probably, the enzyme might not have encountered the perturbations caused by the additional oxetane-ring in the sugar, which is being located far away from the nucleobase. However, in the case of pyrimidine-oxetane units, the oxetane ring is close to the pyrimidine ring, which might interfere with the enzyme. This is evident in the triple

(27) Fox, K. R. *Methods Mol. Biol.*; Fox, K. R., Ed.; Humana Press Inc.: Totowa, NJ, 1997; Vol. 90, p 1.
(28) Suck, D. *J. Mol. Recognit.* **1994**, *7*, 65.
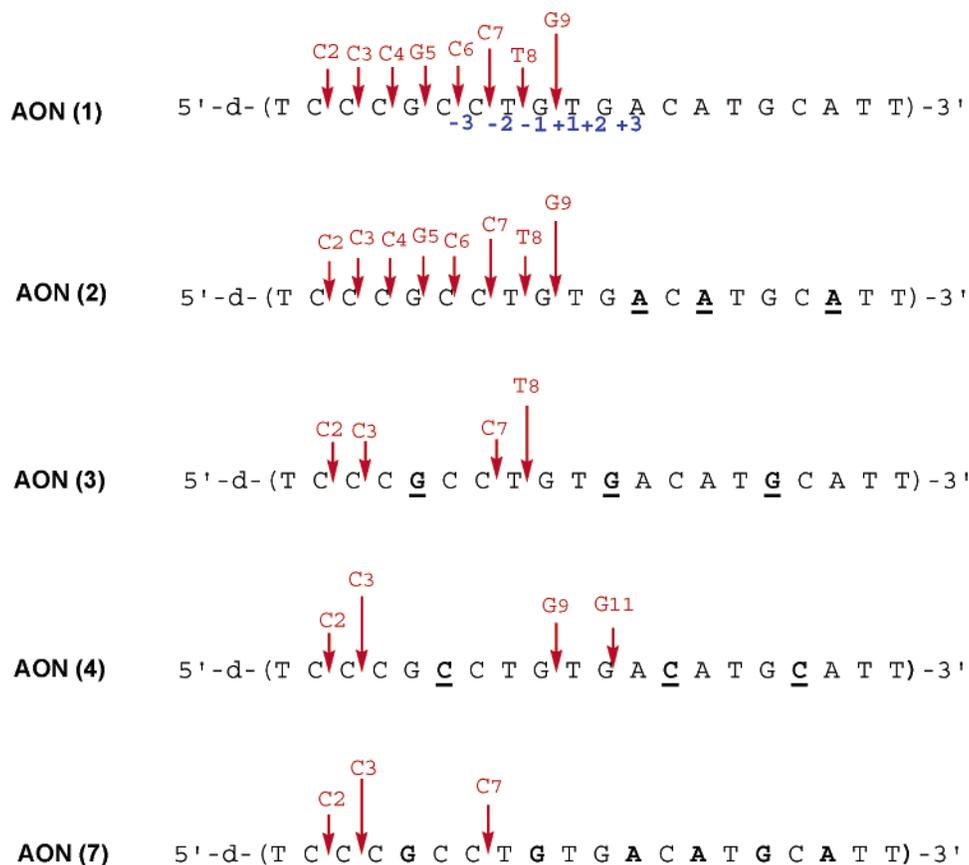(29) Herrera, J. E.; Chaires, J. B. *J. Mol. Biol.* **1994**, *236*, 405.

Figure 3. Cleavage pattern of the DNase 1 degradation of AON (**1**)−(**4**) and (**7**) by the PAGE analysis. The % of AON left after 4 h of incubation: 0% of AON (**1**), 0% of AON (**2**), 0% of AON (**3**), 50% of AON (**4**), and 30% of AON (**7**). The vertical arrows show the DNA cleavage sites and the relative length of an arrow shows the relative extent of cleavage at that site.

oxetane-C modified AON (**4**), where only minor cleavage was observed at the G9 along with the G11 while the major cleavage was observed at the C3 and it is very close to the 5′-end. However, the rate of cleavage was low at those sites probably owing to the perturbations of the AON-enzyme interaction by the oxetane-C, which is situated just three nucleotide away from the cleavage site. The AON (**7**) incorporated with **6** oxetane-purines has shown a half-life of the cleavage the cleavage to be about 2 h. These results lead us to suggest that to get effective endonuclease resistance with the oxetane-purine units, extensive (probably every alternate nucleotide) modifications of the AON strand are needed. This, however, may slow the RNase H recruiting capability (vide infra). Another viable approach can be the use of a mixture of the oxetane-purines and a minimum amount of the oxetane-pyrimidines.

To investigate the tolerance of the oxetane-modifications toward an exonuclease (snake venom phosphodiesterase, SVPDE), we have synthesized an AON (**12**) with 3 consecutive oxetane-**C**, -**A**, and -**G** units at the 3′-end. Incubation with the SVPDE showed that the presence of the oxetane-modified units at the 3′-end offers resistance toward cleavage: 36% of AON (**12**) was left after 24h incubation with the enzyme, while the native PO-AON (**1**) was completely degraded in less than 2 h of incubation (Figure S3 in Supporting Information). The same AON showed half-life of around 9 h in human blood serum where major degrading enzymes are exonucleases (Figure S4 in Supporting Information). Complete exonuclease protection was achieved in case of the 3′-DPPZ conjugated AONs (**8** and **9**, (Figure S3 in Supporting Information), which were found to

have slightly better stability than the native PS-AON in human serum (Figure S4 in Supporting Information).

(D) RNase H1 Cleavage Pattern of the Complementary RNA and the Extent (%) of RNA Cleavage in Hetero-duplexes Containing Oxetane-*A*, -*G*, -*C* Units and Their DPPZ Conjugates. All of the oxetane-*A* and -*G* modified AON (**2-7**)/RNA (**13**) hybrids and their DPPZ conjugates (**8** and **9**) were found to be substrates for the *Escherichia coli* RNase H1 with varying cleavage potential. In the RNase H1 cleavage pattern of all the oxetane-*A* and -*G* modified AON/RNA hybrids, except for the AON (**7**)/RNA (**13**), a region of 5 nucleotides in the RNA strand toward the 3′-end from the site opposite to the oxetane modification, was found to be resistant toward RNase H promoted cleavage (Figures 4 and 5). This is presumably owing to the local steric and structural alterations brought about by the modification, thereby preventing the flexibility and accessibility required for the RNase H cleavage.[3] This *5-nucleotide footprint* is identical to what was found earlier for the oxetane-*T* and -*C* modified AON/RNA hybrids.[22−24] The cleavage of the AON (**7**)/RNA (**13**) at A11 site was surprising because this cleavage site is located within the anticipated footprint region of the oxetane-*A* modification (Figure 4).

Our earlier studies of the oxetane-*T* and -*C* modified AON/RNA hybrids revealed that the RNase H cleavage potentials of these modified hybrids depend on the concentration of the RNA as a substrate.[22b,23,24] This has prompted us to test all our modified AONs at two different substrate (RNA) concentrations. We have deduced the extent of cleavage at high (0.8 μM) and low (0.01 μM) RNA concentrations (Figure 6) under saturation
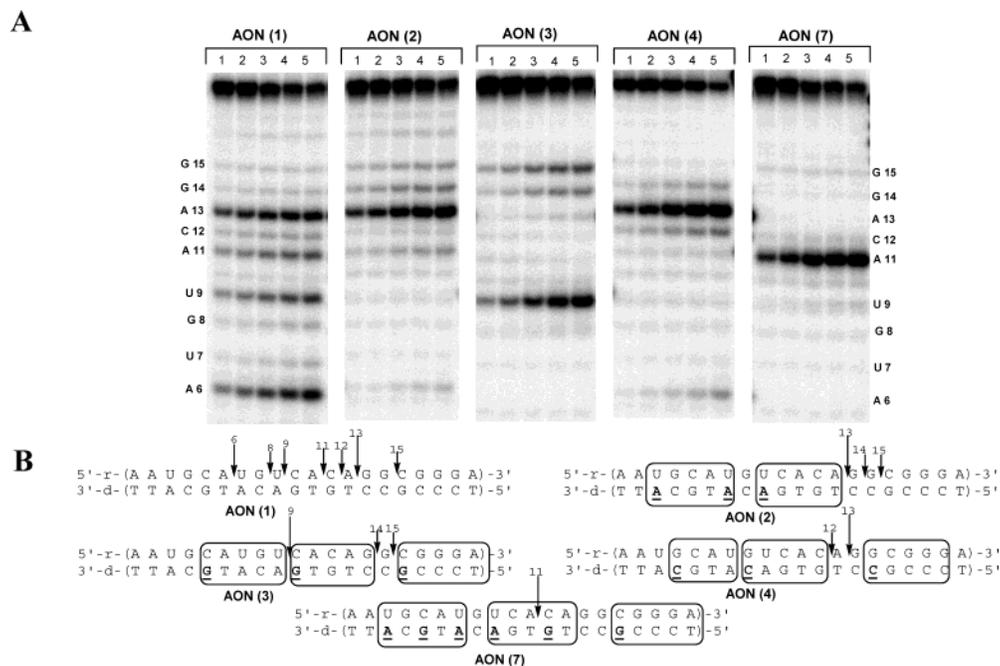
Figure 4. (A) Autoradiograms of 20% denaturing PAGE, showing the cleavage kinetics of 5′-^{32}P-labeled target RNA (**13**) by *E. coli* RNase H1 in the native AON (**1**)/RNA (**13**) and the oxetane-*A*, -*G*, and -*C* modified AON (**2**−**4** and **7**)/RNA (**13**) hybrid duplexes. Lanes 1 to 5 represent the aliquots of the digest taken after 5, 10, 15, 30, and 60 min, respectively. Conditions of cleavage reaction: RNA (0.8 μM) and AONs (4 μM) in buffer, containing 20 mM Tris-HCl (pH 8.0), 20 mM KCl, 10 mM MgCl$_2$ and 0.1 mM DTT at 21 °C; 0.8 U of RNase H. Total reaction volume was 30 μL. The % of RNA left intact after 1 h of incubation: 28% for AON (**1**), 36% for AON (**2**), 50% for AON (**3**), 26% for AON (**4**) and AON for 32% (**7**). (B) RNase H1 cleavage pattern of hybrid duplexes. The vertical arrows show the RNA cleavage sites and relative length of an arrow shows the relative extent of cleavage at that site.
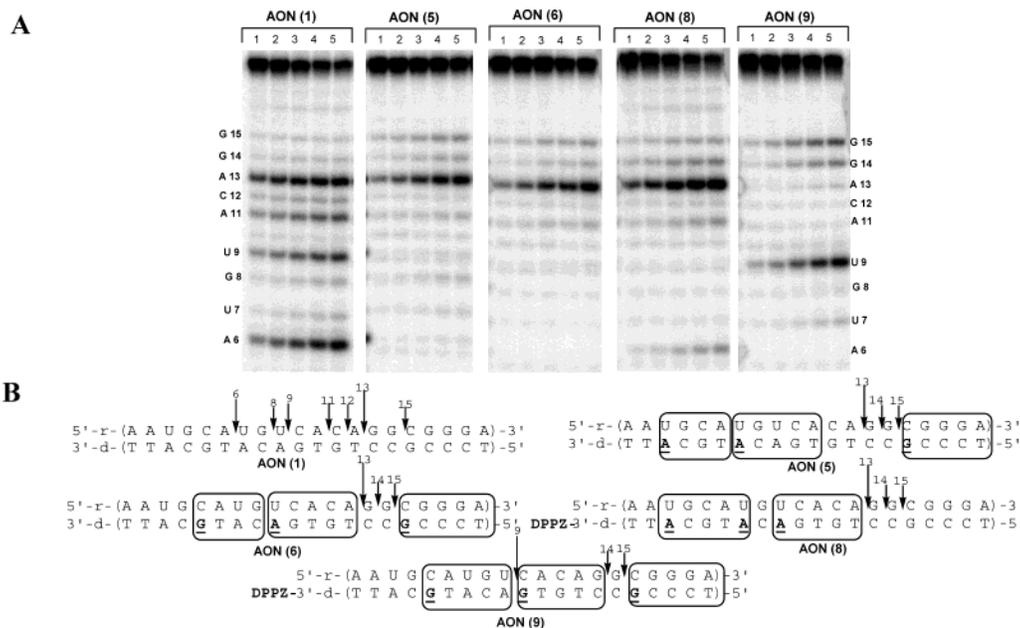

Figure 5. (A) Autoradiograms of 20% denaturing PAGE, showing the cleavage kinetics of 5′-^{32}P-labeled target RNA (**13**) by *E. coli* RNase H1 in the native AON (**1**)/RNA (**13**) and the oxetane-*A*, -*G*, and -*C* modified AON (**5**, **6**, **8**, and **9**)/RNA (**13**) hybrid duplexes. Lanes 1 to 5 represent the aliquots of the digest taken after 5, 10, 15, 30, and 60 min respectively. Conditions of the cleavage reaction: RNA (0.8 μM) and AONs (4 μM) in buffer, containing 20 mM Tris-HCl (pH 8.0), 20 mM KCl, 10 mM MgCl$_2$ and 0.1 mM DTT at 21 °C; 0.8 U of RNase H. Total reaction volume was 30 μL. The % of RNA left after 1h of incubation: 34% for AON (**1**), 65% for AON (**5**), 64% for AON (**6**), 37% for AON (**8**) and 64% for AON (**9**). (B) RNase H cleavage pattern of hybrid duplexes. The vertical arrows show the RNA cleavage sites and relative length of an arrow shows the relative extent of cleavage at that site.

conditions (the enzyme is completely saturated by the substrate). At the low RNA concentration, the triple oxetane-*A* (**2**) and triple oxetane-*G* (**3**) modified AON/RNA hybrid duplexes and their respective DPPZ counterparts (**8**) and (**9**) have shown the extent of the cleavage slightly lower than that of the native AON (**1**)/RNA (**13**) hybrid duplex (Figure 6). The mixed *A* and *G* incorporated AON (**5** and **6**)/RNA (**13**) hybrids have also shown

similar cleavage characteristics. Exception was found for the AON (**7**)/RNA (**13**), incorporated with 6 oxetane−purine moieties, where the extent of cleavage was extremely low (17 ± 3%) compared to that of the native AON (**1**)/RNA (**13**) hybrid duplex. It should be noted that under these conditions the triple oxetane-*C* modified AON (**4**)/RNA (**13**) hybrid duplex has shown a comparable or slightly better extent of cleavage (78 ±
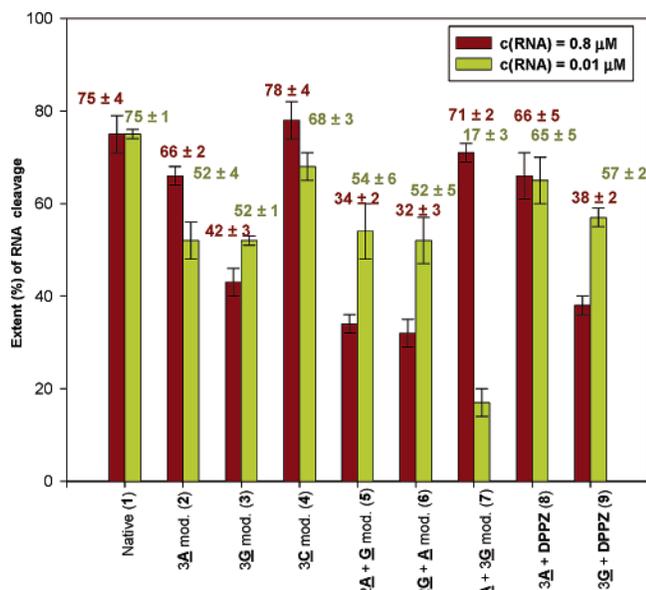
Figure 6. Bar graphs showing the extent (%) of the *E. coli* RNase H1 promoted target RNA (**13**) hydrolysis in AON/RNA hybrid duplexes after 1 h incubation with the enzyme for native 20mer AON (**1**) and the oxetane-*A*, -*G*, and -*C* modified AONs (**2**–**9**) at high (0.8 μM) and low (0.01 μM) substrate (RNA) concentration. Conditions of cleavage reactions: RNA (0.01 or 0.8 μM) and AONs (4 μM) in buffer, containing 20 mM Tris-HCl (pH 8.0), 20 mM KCl, 10 mM MgCl$_2$ and 0.1 mM DTT at 21 °C; 0.08 U of RNase H for reactions under low RNA concentration and 0.8 unit of enzyme for reactions under high RNA concentration. Total reaction volume was 30 μL.
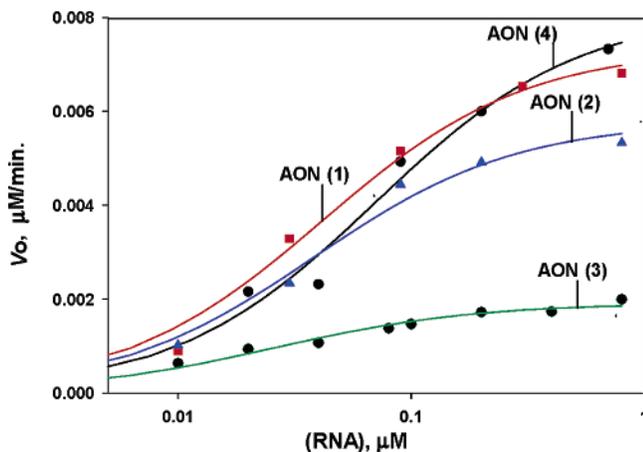

Figure 7. Initial velocity of the hydrolysis (v_o) of the 20mer target RNA (**13**) in the AON (**1**–**4**)/RNA hybrids (see Figure 2) by *E. coli* RNase H as a function of the RNA concentration (logarithmic scale). Conditions of the cleavage reaction: AONs (4 μM) and RNA (**13**) in buffer containing 20 mM Tris-HCl (pH 8.0), 20 mM KCl, 10 mM MgCl$_2$ and 0.1 mM DTT at 21 °C, 0.08 U of RNase H. Total reaction volume was 30 μL.

1%) than that of the native hybrid duplex (75 ± 1%). These data clearly show that the triple oxetane-*A* and triple oxetane-*G* modified AON/RNA hybrids are capable of recruiting RNase H in an efficient manner (52–60% of RNA was cleaved) at low substrate concentrations, and it is important in view of extremely low concentrations of target mRNAs in many infected cells.[30]

At high substrate concentration (0.8 μM RNA), the hybrid duplexes of the triple oxetane-*A* modified AON (**2**) and its DPPZ counterpart (**8**) showed the extent of cleavage comparable to that of the native (**1**) and triple *C* (**4**) modified AON/RNA hybrids (Figure 6) However, the hybrid duplexes of the triple
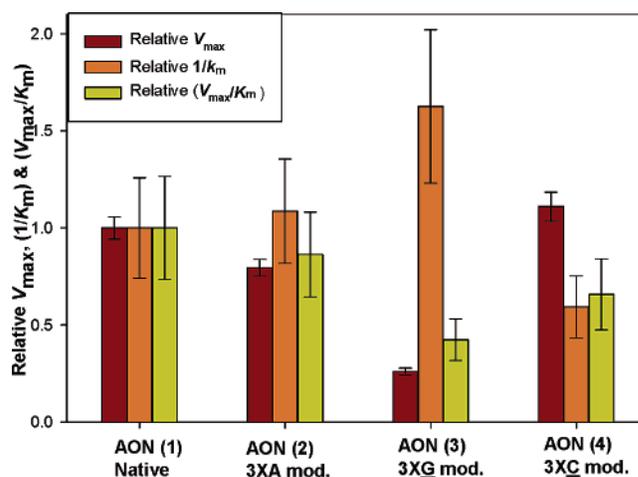
Figure 8. Bar graphs showing the relative (with respect to the native AON) V_{max}, $1/K_m$ and V_{max}/K_m values for the RNase H promoted RNA hydrolysis in AON/RNA hybrid duplexes (Figure 2) formed by the native 20mer AON (**1**), oxetane-*A*, -*G*, and -*C* modified AONs (**2**–**4**).

oxetane-*G* modified AON (**3**), its 3′-DPPZ containing counterpart (**9**) and the AONs (**5** and **6**) containing both the oxetane-*A* and oxetane-*G* units have shown relatively low cleavage by the RNase H (Figure 6). Surprisingly, the AON (**7**)/RNA (**13**) hybrid, which had shown very low cleavage at low RNA concentration, showed RNase H cleavage close to that of the native hybrid duplex. This underscores the differential cleavage characteristics of the oxetane-purine modified AON/RNA hybrids at different substrate concentrations.

(E) Michaelis–Menten Kinetics of the Oxetane-*A* and -*G* Modified AON/RNA Hybrids and Their Comparison with the Oxetane-*C* and Native AON/RNA Hybrid Duplexes. To obtain a deeper understanding of the *E. coli* RNase H1 recognition and cleavage of the oxetane-*A* and -*G* modified AON (**3** and **4**)/RNA (**13**) hybrids, a detailed Michaelis–Menten kinetics has been carried out and the kinetic parameters were subsequently compared with those of the native (**1**) and the triple oxetane-*C* modified AON (**4**)/RNA (**13**) hybrids (Table 2, Figures 7 and 8).

It is evident from the kinetic data that the triple oxetane-*A* modified AON (**2**)/RNA (**13**) duplex has a maximum velocity, V_{max}, slightly lower than that of the native (**1**) and the triple oxetane-*C* modified AON (**4**)/RNA (**13**) hybrids. However, its enzyme binding affinity, $1/K_m$, has found to be very close to the native yielding an effective enzyme activity, k_{cat}/K_m, close to that of the native. The triple oxetane-*G* modified AON (**3**)/RNA (**13**) has shown a lower V_{max} and K_m value compared to those of the native, triple oxetane-*A* and the triple oxetane-*C* modified AON/RNA hybrids (Table 2, Figures 7 and 8). Thus, the k_{cat}/K_m value of oxetane-*G* modified AON (**3**)/RNA (**13**) is half of that of the native AON (**1**)/RNA (**13**) duplex. Noteworthy the fact that the V_{max} value appeared to be higher for the triple oxetane-*C* modified AON/RNA duplex than for the native (Table 2, Figures 7 and 8). This can be attributed the lower binding affinity ($1/K_m$) and lower T_m of the triple *C* modified AON/RNA duplex similar to the observations made in our previous studies on various oxetane-*C* and -*T* modified 15mer AON/RNA hybrids.[23,24] The reason for the lower V_{max} and high $1/K_m$ of the triple oxetane-*G* modified AON/RNA duplex is not

(30) Baer, M. R.; Augustinos, P.; Kinniburgh, A. *Blood* **1992**, *79*, 1319.

Table 2. Kinetic Characteristics of the RNA Cleavage by *E. coli* RNase H1 of the AON (**1−4**)/RNA (**13**) Hybrid Duplexes

AONs	T_m (°C)	V_{max}, 10^{-3} μM min^{-1}	K_m, 10^{-3} μM	k_{cat}, min^{-1}	(V_{max}/K_m), min^{-1}	(k_{cat}/K_m), μM^{-1} min^{-1}	relative (k_{cat}/K_m)
native 20mer (**1**)	74	7.3 ± 0.3	44.4 ±6.3	24.2 ± 1	0.164	545.1	1
3A-oxetane-modified AON 20−**3A** (**2**)	73	5.8 ± 0.2	38.3 ± 6.4	19.2 ± 0.6	0.15	501.3	0.92
3G-oxetane-modified AON 20−**3G** (**3**)	74	1.9 ± 0.1	25.6 ± 4.1	6.3 ± 0.35	0.074	246.1	0.45
3C-oxetane-modified AON 20−**3C** (**4**)	61	8.1 ± 0.5	70.2 ± 13.8	26.9 ± 1.5	0.11	383.7	0.70

[a] $V_{max} = k_{cat}E_0$ ($E_0 = 0.08$ U/30 μL $= 2.66 \times 10^{-3}$ U/μL $= 3.016 \times 10^{-4}$ μM), specific activity $= 420\,000$ U/mg or 2.38×10^{-6} mg/U $= 1.133\,86 \times 10^{-13}$ mol/unit, MW $= 21\,000$ g/mol.

Scheme 1 [a]
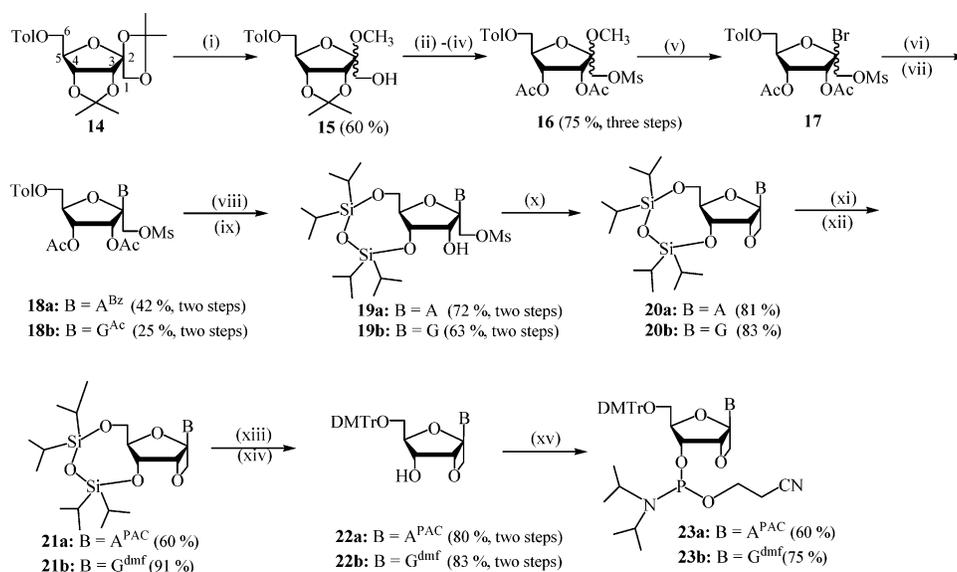
[a] Reagents and conditions: (i) 0.4 M methanolic HCl, r.t., 12 h; (ii) MsCl, pyridine, 4 °C, 12 h; (iii) 90% TFA/water, r.t., 20 min (iv) acetic anhydride, pyridine, r.t., 3 h; (v) 30% HBr/AcOH, 0 °C to r.t., 12 h; (vi) persilylated N^6-benzoyl-adenine, CH$_3$CN, SnCl$_4$, 70 °C, 4 h, r.t., 12 h for **18a**; (vii) persilylated N^2-acetyl-O^6-diphenylcarbamoylguanine, CH$_3$CN-DCE, SnCl$_4$, 70 °C, 5 h, r.t., 12 h followed by 90% TFA/water, r.t., 20 min for **18b**; (viii) methanolic NH$_3$, r.t., 48 h; (ix) TIPDS−Cl$_2$, pyridine, 4 °C, 30 min, r.t., 2 h; (x) NaHMDS, THF, 4 °C, 2 h; (xi) PAC−Cl, pyridine, 4 °C, 2 h., r.t., 2 h for **21a**; (xii) N,N-dimethylformamide dimethylacetal, MeOH, r.t., 12 h for **21b**; (xiii) 1M TBAF, THF, r.t., 4 min; (xiv) DMTrCl, pyridine, r.t., 12 h; (xv) (2-cyanoethoxy)bis(N,N-diisopropylamino)phosphine, N,N-diisopropylammonium tetrazolide, DCM, r.t., 2 h. Abbreviations: Tol = 4-methylbenzoyl, r.t. = room temperature, Ms = methanesulfonyl, TFA = trifluoroacetic acid, Ac = acetyl, DCE = dichloroethane, TIPDS = 1,1′,3,3′-tetraisopropyldisiloxane-1,3-diyl, NaHMDS = sodium bis(trimethylsilyl) amide, PAC = phenoxyacetyl, TBAF = tetrabutylammonium fluoride, THF = tetrahydrofuran, DMTr = 4,4′-dimethoxytrityl, DCM = dichloromethane.

clear. Clearly, more modified sequences have to be tested before drawing any general conclusions regarding the RNase H recruitment by the oxetane-**G** and -**A** modified AON/RNA hybrids.

(F) Synthesis of the Oxetane-*A* and -*G* Building Blocks. The oxetane-**A** and oxetane-**G** phosphoramidites, **23a** and **23b**, required for incorporation into AONs (**2−9** and **12**) were synthesized using a strategy shown in Scheme 1. The synthesis started with the conversion of 6-*O*-(4-toluoyl)-1,2:3,4-diisopropylene-β-D-psicofuranose (**14**),[22b] into **16**, a possible key intermediate in the nucleobase coupling, using a reported procedure.[31] It is noteworthy that some yields obtained in our hands were significantly lower in certain steps compared to that reported earlier.[31] Thus, the transformation from **14** to **15** (Scheme 1) yielded in only 60% compared to the 91% reported.[31] Since the attempts to couple the silylated purine nucleobase derivatives with **16** were unsuccessful, we have decided to transform **16** into the bromosugar **17** followed by immediate coupling of the crude **17** with the silylated N^6-

(31) Roivainen, J.; Vepsalainen, J.; Azhayev, A.; Mikhailopulo, I. A. *Tetrahedron Lett.* **2002**, *43*, 6553.

benzoyladenine and N^2-acetyl-O^6-diphenylcarbamoylguanine in the presence of SnCl$_4$ as Lewis acid catalyst. This afforded the β-nucleosides **18a**; and yielded **18b** (together with the short treatment with TFA to remove the DPC: 25%). The yield of two step transformation from **16** to **18** was 42% compared to 95% reported.[31] Along with **18a** we got very little amount of α anomers with a lot of nonnucleosidic impurities. This has reduced the overall yield. For **18b** we got inseparable mixtures of N7 α and β nucleosides along with inseparable mixtures of N9 (both α and β) and N7 (both α and β) psiconucleosides without the DPC protection. Moreover, there also were non-nucleosidic impurities. Unfortunately, due to the use of repeated columns for purification we could not quantify the yields of all those side products. The β configurations of the products were determined by NOE measurements. NOE observed between H-8 and H-3′, which are separated by 1.9 Å, in **18a** was 2%. In the case of **18b** NOE between H-8 and H-3′, was found to be 2.7%. Such kind of NOE cannot be observed in the α anomers owing to the 3.9 Å distance between H-8 and H-3′. The N9-connectivity of the base in **18b** was evidenced by the chemical shift of C5 of the base at 122.0 ppm in the ^{13}C NMR spectra,
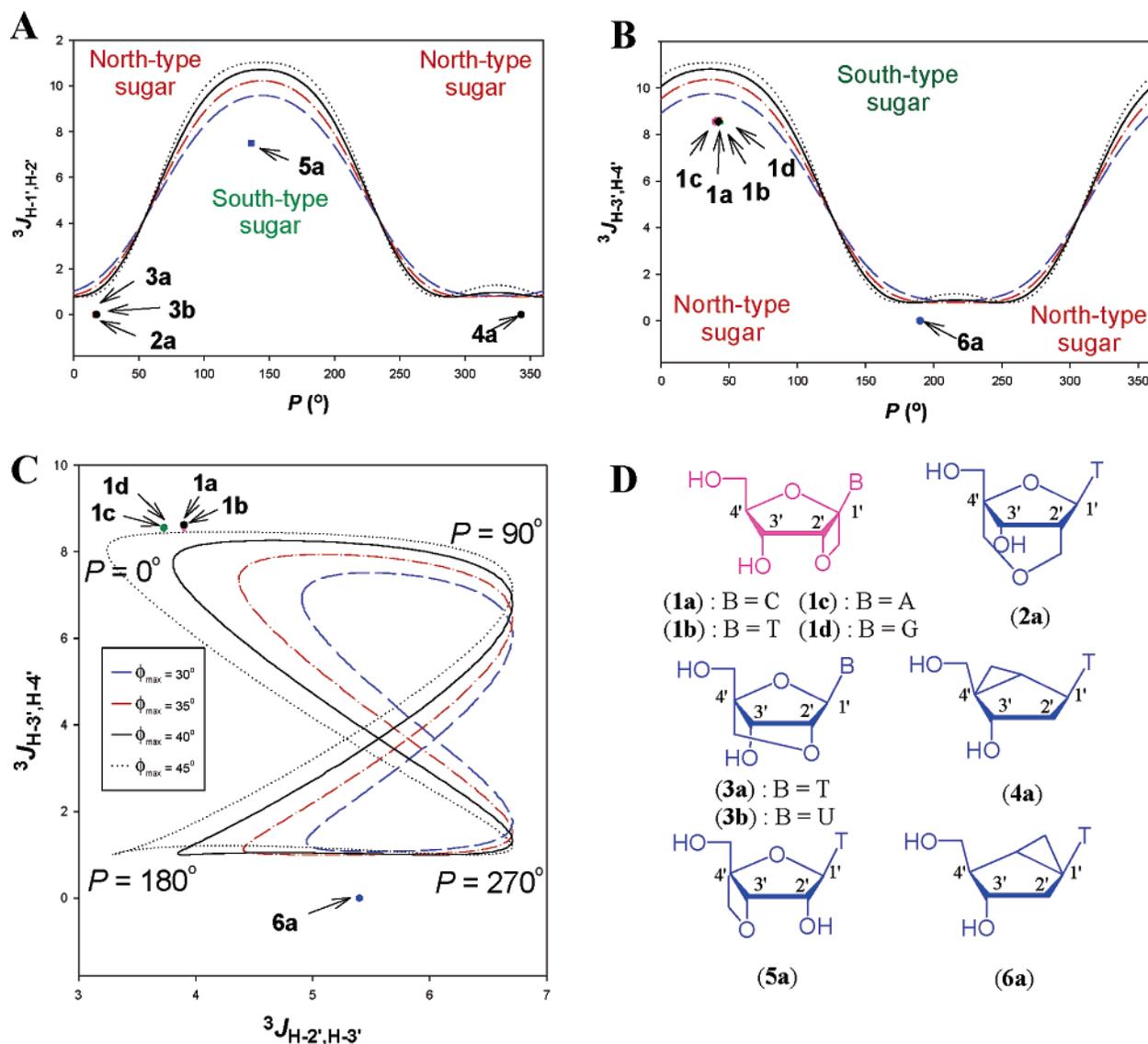
Figure 9. Calculated and experimental values of the $^3J_{H,H}$ vicinal proton coupling constants (Hz) (see Table S1 in Supporting Information). Theoretical dependences (color lined in frames (**A**)−(**C**)) of the $^3J_{H,H}$ were calculated by varying the phase angle of pseudorotation (*P*) from 0° to 360° using generalized Karplus-type equation ($P_1 = 13.24$, $P_2 = -0.91$, $P_3 = 0$, $P_4 = 0.53$, $P_5 = -2.41$, $P_6 = 15.5°$) developed by Altona et al.[36] at fixed puckering amplitudes of 30° (blue dashed line), 35° (red dot−dashed line), 40° (black line), and 45° (black dotted line). The experimental coupling constants for the oxetane-modified nucleosides (**1a**)−(**1d**) were obtained through 600 MHz ^1H NMR spectra (DMSO-d_6 + CD$_3$OD) at 298 K. The experimental coupling constants of the *North*-type sugar (**2a**),[38] (**3a**),[39] (**3b**),[16e] and (**4a**)[16b] and the *South*-type sugar (**5a**)[40] and (**6a**)[42] compounds are presented from available NMR and X-ray data. Note that the numbering of the sugar atoms used in this figure differs from the nomenclature defined numbering (Scheme 1) employed throughout the paper.

which is a characteristic for the N9-isomer.[32] Methanolysis of **18a**−**b** followed by simultaneous protection of 4′ and 6′ hydroxyl groups using 1,3-dichloro-1,1′,3,3′-tetraisopropyl-disiloxane (TIPDSCl$_2$) furnished the precursors, **19a** (72%) and **19b** (63%), required for the oxetane ring formation. The cyclization was achieved by the treatment of **19a**−**b** with NaHMDS in THF at 4 °C, giving **20a** (81%) and **20b** (83%). The exocyclic amino group of the **20a** was protected by phenoxyacetyl group and that of **20b** by dimethylformamidine group to furnish **21a** (60%) and **21b** (91%). The removal of the TIPDS group from **21a**−**b** followed by one-pot dimethoxy-tritylation afforded **22a** (80%) and **22b** (83%). Compounds **22a**−**b** were transformed to their corresponding phosphor-amidites **23a** (60%) and **23b** (75%), the building blocks required for the solid-phase synthesis of the modified AONs (**2**−**9** and **12**).

(32) Garner, P.; Ramakanth, S. *J. Org. Chem.* **1988**, *53*, 1294.

(G) Conformational Analysis of the Oxetane-Fused Sugar Moiety. Conformational Analysis Based on Experimental $^3J_{H,H}$ Coupling Data. The conformation adopted by the pentose in the bicyclic (1′,3′-O-anhydro-β-D)-furanosyl oxetane-modified nucleosides (compounds **1a**−**1d** in Figure 9, frame **D**), is not possible to estimate directly from the vicinal proton−proton coupling constants due to the lack of an important endocyclic $^3J_{H-2',H-3'}$ ($^3J_{H-1',H-2'}$ in Figure 9) coupling. But a fair amount of information about this conformation can be extracted from the experimental $^3J_{H-3',H-4'}$ and $^3J_{H-4',H-5'}$ (referred to as $^3J_{H-2',H-3'}$ and $^3J_{H-3',H-4'}$ in Figure 9) coupling constants. Using generalized Karplus-type equation developed by Altona et al.,[36,37] a set of empirical rules relating $^3J_{H,H'}$ coupling constants of pentose can be used in analysis of the vicinal couplings. It is well established that a high or low value of the $^3J_{H-1',H-2'}$ in conjunction with a low or a high value of $^3J_{H-3',H-4'}$, respec-

Table 3. Proton Chemical Shifts (δ Scale, ppm) and $^3J_{H,H}$ Coupling Constants (Hz) for the Oxetane-**C** (**1a**),[a] -**T** (**1b**),[a] -**A** (**1c**), and -**G** (**1d**) (^{1}H NMR spectra were recorded in DMSO-d_6 with methanol-d_4 at 600 MHz using DMSO-d_6 (2.6 ppm) peak as internal standard)

	Oxetane-**A** (1c)	Oxetane-**G** (1d)	Oxetane-**C** (1a)	Oxetane-**T** (1b)
H1′	5.55 (d, J_{gem} = 7.9 Hz)	5.42 (d, J_{gem} = 8.0 Hz)	5.07 (d, J_{gem} = 8.15 Hz)	5.11 (d, J_{gem} = 8.15 Hz)
H1″	4.96 (d)	4.88 (d)	4.67 (d)	4.68 (d)
H3′	5.63 (d, $J_{H-3',H-4'}$ = 3.73 Hz)	5.53 (d, $J_{H-3',H-4'}$ = 3.73 Hz)	5.30 (d, $J_{H-3',H-4'}$ = 3.9 Hz)	5.36 (d, $J_{H-3',H-4'}$ = 3.9 Hz)
H4′ & H5′	4.37-4.32 (m, $J_{H-4',H-5'}$ = 8.55Hz, $J_{H-5',H-6'}$ = 5.3 Hz)	4.31-4.26 (m, $J_{H-4',H-5'}$ = 8.55 Hz, $J_{H-5',H-6'}$ = 5.7 Hz)	4.19-4.12 (m, $J_{H-4',H-5'}$ = 8.55 Hz, $J_{H-5',H-6'}$ = 5.9 Hz)	4.19-4.13 (m, $J_{H-4',H-5'}$ = 8.62 Hz, $J_{H5',H6'}$ = 5.8 Hz)
H6′	3.91 (dd, J_{gem}=12.3, $J_{H-5',H-6'}$ = 1.75 Hz)	3.89 (dd, J_{gem}=12.3 Hz, $J_{H-5',H-6'}$ = 1.76 Hz)	3.85 (d, J_{gem}= 12.2, $J_{H-5',H-6'}$ = 1.78 Hz)	3.85 (dd, 12.3 Hz, $J_{H-5',H-6'}$ = 1.87 Hz)
H6″	3.66 (dd)	3.66 (dd)	3.59 (dd)	3.60 (dd)
H2/H5	8.39 (s, H-2)	-	5.84 (d, $J_{H-5,H-6}$= 7.373 Hz, H-5)	-
H8/H6	8.25 (s, H-8)	7.92 (s, H-8)	7.47 (d, H-6)	7.42 (d, 1.28 Hz, H-6)
CH$_3$	-	-		1.94 (d)

[a] The ^{1}H NMR data for the oxetane-**C** (**1a**) in D$_2$O and the oxetane-**T** (**1b**) in methanol-d_4 have been reported in refs 24 and 22b, respectively.

tively, are considered to be strong indicators of the *South-* or the *North*-type conformation (see the $^3J_{H-1',H-2'}$ and $^3J_{H-3',H-4'}$ dependencies on the pseudorotational phase angle *P* in frames **A** and **B** in Figure 9) as it is shown for the typical *North*-type conformation for compounds **2a** ($^3J_{H-1',H-2'}$ = 0.0 Hz, *P* = 16.5°),[38] **3a** ($^3J_{H-1',H-2'}$ = 0.0 Hz, *P* = 17°),[39] **3b** ($^3J_{H-1',H-2'}$ = 0.0 Hz, *P* = 17.4°),[16e] **4a** ($^3J_{H-1',H-2'}$ = 0.0 Hz, $^3J_{H-1',H-2''}$ = 6.8 Hz, *P* = 343°)[16b] and the typical *South*-type conformation for compounds **5a** ($^3J_{H-1',H-2'}$ = 7.5 Hz, $^3J_{H-2',H-3'}$ = 0.0 Hz, *P* = 136°)[40] and **6a** ($^3J_{H-2',H-3'}$ = 3.0 Hz, $^3J_{H-2'',H-3'}$ = 5.4 Hz, $^3J_{H-3',H-4'}$ = 0.0 Hz, *P* = 190°)[42] (molecular structures and atom numbering are shown in Figure 9, frame **D**).

The $^3J_{H-3',H-4'}$ coupling ($^3J_{H-4',H-5'}$ in the nomenclature of the oxetane-modified nucleotides) of >~8 Hz, along with $^3J_{H-1',H-2'}$ of <~1.5 Hz, would indicate that the pentose-sugar is locked in the *North*-type conformation (Figure 9, frame **B**) and, in contradistinction, a $^3J_{H-3',H-4'}$ < ~1.0 Hz and $^3J_{H-1',H-2'}$ of >~8 Hz would finger-point a constrained *South*-type conformation (the exact limits depend on the electronegativity of the substituents and the substitution pattern)[36,37,41] Thus, a $^3J_{H-3',H-4'} \approx 0$ Hz for the compound **6a** alone indicates the *South*-type structure (Figure 9, frame **D**) which agrees with its available X-ray structure.[42] The $^3J_{H-4',H-5'}$ values of the oxetane-modified compounds **1a**–**1d** (Figure 9, frame **D**) are ~8.6 Hz (Table 3) which leads to conclusion that the sugar moieties of the oxetane-**C**, -**T**, -**A**, and -**G** nucleosides are locked in the *North*-type conformation. The dependence $^3J_{H-2',H-3'}$ versus

$^3J_{H-3',H-4'}$ (frame **C**, Figure 9) shows the combination of these coupling constants for the oxetane-modified nucleosides to be typical for *P* = 20−60° range which unambiguously points to the *North*-conformation as opposed to *South*-type conformation for compound **6a** (Figure 9, frames **C** and **D**). The $^3J_{H-2',H-3'}$ and $^3J_{H-3',H-4'}$ (see numbering in Figure 9) of the oxetane-**C**, -**T**, -**A**, and -**G** nucleosides have been found to be temperature-independent, thus the ^{1}H NMR data suggest that the sugar moiety of the oxetane-modified nucleosides are locked in the *North*-type conformation.[16e−f,16h,43,44]

Ab Initio Calculations. In an alternative analysis, the ab initio geometry optimizations for each of the oxetane modified nucleosides **1a**−**1d** (Figure 9, frame **D**) were performed to obtain the geometrical parameters. It was followed by the 0.5 ns MD simulations in the explicit aqueous medium to probe a conformational hyperspace available for these systems. The ab initio calculations utilizing 6-31G* Hartree−Fock geometry optimization by Gaussian 98 program[45] resulted in the H3′−C3′−C4′−H4′ and H4′−C4′−C5′−H5′ torsions to be ~43.4° and ~163.5°, respectively and these values varied only by ±0.4° for all the oxetane-**A**, -**G**, -**C**, and -**T** nucleosides **1a**−**1d** (Table S1 in Supporting Information). The positions of the heavy atoms of sugar moieties of the respective oxetane-modified nucleosides vary slightly between the nucleosides resulting in less than 0.01 Å RMS difference as it can clear be seen in Figure 10, frame **A**. The theoretical vicinal coupling constants estimated using these H3′−C3′−C4′−H4′ and H4′−C4′−C5′−H5′ torsions and the generalized Karplus equation[36] agree well with the experimental $^3J_{H,H}$ constants (max RMSd = 0.46 Hz, see Table S1 in

(33) Nielsen, P. E. *Curr. Opin. Mol. Ther.* **2000**, *2*, 282.
(34) Gryaznov, S. M. *Biochim. Biophys. Acta* **1999**, *1489*, 131.
(35) Summerton, J.; Weller, D. *Antisense Nucleic Acid Drug Dev.* **1997**, *7*, 187.
(36) Haasnoot, C. A. G.; DeLeeuw, F. A. A. M.; Altona, C. *Tetrahedron* **1980**, *36*, 2783, and references therein.
(37) Altona, C.; Sundaralingam, M. *J. Am. Chem. Soc.* **1972**, *94*, 8205, and references therein.
(38) Wang, G.; Gunic, E.; Girardet, J.-L.; Stoisavljevic, V. *Bioorg. Med. Chem. Lett.* **1999**, *9*, 1147.
(39) Nielsen, C. B.; Singh, S. K.; Wengel, J.; Jacobsen, J. P. *J. Biomol. Struct. Dyn.* **1999**, *17*, 175.
(40) Obika S.; Morio, K.-i.; Hari, Y.; Imanishi, T. *Chem. Commun.* **1999**, 2423.
(41) Thibaudeau, C.; Chattopadhyaya, J. *Stereoelectronic Effects in Nucleosides and Nucleotides and their Structural Implications*; Department of Bioorganic Chemistry, Uppsala University Press (jyoti@boc.uu.se): Sweden, 1999 (ISBN 91-506-1351-0).
(42) Altman, K.-H.; Imwinkelried, R.; Kesselring, R.; E.; Rihs, G. *Tetrahedron Lett.* **1994**, *35*, 7625.

(43) Ravn, J.; Nielsen, P. *J. Chem. Soc., Perkin Trans. 1* **2001**, 985
(44) Tarköy, M.; Bolli, M.; Schweizer, B.; Leumann, C. *Helv. Chim. Acta* **1993**, *76*, 481.
(45) Frisch, M. J.; Trucks, G. W.; Schlegel, H. B.; Scuseria, G. E.; Robb, M. A.; Cheeseman, J. R.; Zakrzewski, V. G.; Montgomery, Jr., J. A.; Stratmann, R. E.; Burant, J. C.; Dapprich, S.; Millam, J. M.; Daniels, A. D.; Kudin, K. N.; Strain, M. C.; Farkas, O.; Tomasi, J.; Barone, V.; Cossi, M.; Cammi, R.; Mennucci, B.; Pomelli, C.; Adamo, C.; Clifford, S.; Ochterski, J.; Petersson, G.; Ayala, P. Y.; Cui, Q.; Morokuma, K.; Malick, D. K.; Rabuck, A. D.; Raghavachari, K.; Foresman, J. B.; Cioslowski, J.; Ortiz, J. V.; Baboul, A. G.; Stefanov, B. B.; Liu, G.; Liashenko, A.; Piskorz, P.; Komaromi, I.; Gomperts, R.; Martin, R. L.; Fox, D. J.; Keith, T.; Al-Laham, M. A.; Peng, C. Y.; Nanayakkara, A.; Gonzalez, C.; Challacombe, M.; Gill, P. M. W.; Johnson, B. G.; Chen, W.; Wong, M. W.; Andres, J. L.; Head-Gordon, M.; Replogle E. S.; Pople, J. A. *Gaussian 98*, Revision A.6; Gaussian, Inc.: Pittsburgh, PA, 1998.
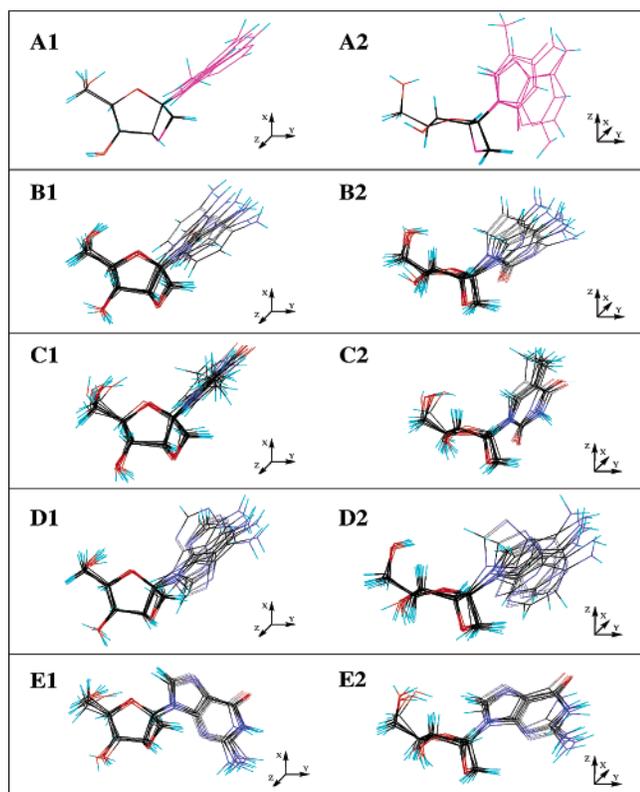
Figure 10. Molecular structures of the oxetane-modified nucleosides shown from the top (**A1**−**E1**) and rotated clockwise by 90° around the *y*-axis (**A2**−**E2**). Projections **A2**−**E2** show that the oxetane-fused sugars are indeed locked in the North-type constrained conformation. Frames (**A1, A2**) show superimposed ab initio optimized geometries of the oxetane-*C* (**1a**), oxetane-*T* (**1b**), oxetane-*A* (**1c**), and oxetane-*G* (**1d**). Frames (**B1, B2**)−(**E1, E2**) contain 10 superimposed molecular structures collected every 10 ps of the last 0.4−0.5 ns interval of the MD simulations of the oxetane-*C* (**B1**, **B2**), oxetane-*T* (**C1**, **C2**), oxetane-*A* (**D1**, **D2**), and oxetane-*G* (**E1**, **E2**), respectively.

Supporting Information). Figure 11 shows that a combination of the experimentally determined $^3J_{H-3',H-4'}$ and $^3J_{H-4',H-5'}$ constants and ab initio obtained values of the respective H3′−C3′−C4′−H4′ and H4′−C4′−C5′−H5′ torsions correlates well with the empirical $^3J_{H,H}$ vs torsion dependence predicted by the Karplus equation, thereby indicating the reliability of the theoretically obtained geometry parameters. The conformation analysis based on the values of the sugar torsion from the ab initio geometries collected in Table 4 for all the oxetane-modified nucleosides reveals that the furanose ring is locked in the *North-East*-type conformation with the phase angle of 40−43° and the puckering amplitude 35−37°.

Molecular dynamics simulations (details are in the Experimental section below) clearly demonstrated that the oxetane ring is firmly restricting the dynamics of the oxetane-fused furanose ring within the typical *North-East*-type ($16° < P < 56°$, $23° < \phi_m < 41°$) conformation range (Table 4) with the average values $30.6° < P < 36.6°$ and $31.7° < \phi_m < 32.7°$ somewhat lower than the corresponding values from the ab initio geometries ($39.8° < P < 42.8°$, $35.1° < \phi_m < 36.6°$) (Table 4). Ten snapshots of the last 100 ps of the MD trajectory (harvested at every 10 ps) are superimposed from the respective MD simulations of the oxetane-modified nucleosides (Figure 10, frames from **B1**, **B2** to **E1**, **E2**). This shows that that the oxetane-fused furanose ring is indeed rigid and locked in to *North-East*-type conformation (shown in Figure 10, projections

B2−**E2**) with the average RMSd being max 0.10 ± 0.03 Å along the trajectories and the major movements are observed for the aglycon part of the oxetane- modified nucleosides (Figure 10, frames from **B1**, **B2** to **E1**, **E2**).

(H) Lessons for Future Design of AONs of Therapeutic Potentials. To show bona fide antisense action the AONs should fulfill broad spectrum of requirements. These include sequence specificity, high exo and endonuclease resistance, RNase H recruitment capability, deliverability, low toxicity, and favorable pharmacokinetics. Achieving all of these goals in a balanced manner by chemical modification of AONs has indeed proven to be a challenging task. The off-target effects and nonantisense properties associated with phosphorothioate AONs[5] pose serious concerns over its therapeutic utilities. Other backbone modifications such as PNA,[33] N3′−P5′ phosphoramidates[34] and morpholino AONs[35] were less specific and unable to activate RNase H degradation of the target RNA. *Hence, any potential modifications without altering the phosphodiester backbone of AONs have been opted as a viable alternative.* Among these, the modifications of the sugar moieties of the nucleosides have been intensively pursued in recent years. However, the loss of RNase H action by extensive modifications of carbohydrate residues such as 2′-*O*-CH$_3$,[9] 2′-*O*-CH$_2$−CH$_2$−O−CH$_3$,[9] 2′-*O*-CH$_2$−CH$_2$−CH$_2$−NH$_2$,[7,10] LNA[16f] etc. in an oligochain limits the antisense potential of these constructs. The "gapmer" design,[7] utilizing such modifications at the ends of the oligo chain and keeping a long stretches of 6−8 unmodified residues, was helpful to partly or fully regain the RNase H recruitment. But such designs will probably be less effective in invoking the antisense action in vivo considering the endonuclease vulnerability observed for some of these gapmers.[21] A recent report[20] showed the utility of α-L-LNA to partly circumvent this problem. A state-of-the-art design would consist of a minimum number of modifications and a maximum antisense action using a minimum amount of antisense reagent, which can only be exploited by employing the catalytic cleavage property of RNase H. Our studies with the oxetane-*C* modified mixmer AONs have proven to be in the right direction toward achieving these goals.[26] We have demonstrated recently in a cellular system the effective down-regulation of the target RNA using the oxetane-*C* modified AONs conjugated with the nontoxic DPPZ group.[26] The fully phosphodiester AONs of such design were in fact ~5 to 6 times more effective in target silencing than the corresponding phosphorothioate AONs.[26] One inherent problem with the oxetane-*C* modified AONs was the loss of thermodynamic stability associated with the modification, even though it has partly or fully been regained by the DPPZ conjugation to short oligomer sequences. The loss of the target affinity can be bypassed by modifications of AONs by the oxetane-*A* and oxetane-*G* units, as reported here. The oxetane-modified AONs, unlike many other conformationally constrained nucleic acids, require only 4 nucleotide gaps to achieve efficient target cleavage by RNase H. Since the flexibility of AON/RNA hybrids is perhaps decisive in dictating their RNase H cleavage rates,[3] it is particularly important that three to four oxetane modifications do not hamper the hybrid flexibility required for the RNase H cleavage, as it is shown in our studies. At low RNA concentration (10 nM) both the oxetane-*A* and -*G* modified AONs and their DPPZ conjugates were found to be good substrates for RNase H with extent of cleavage comparable
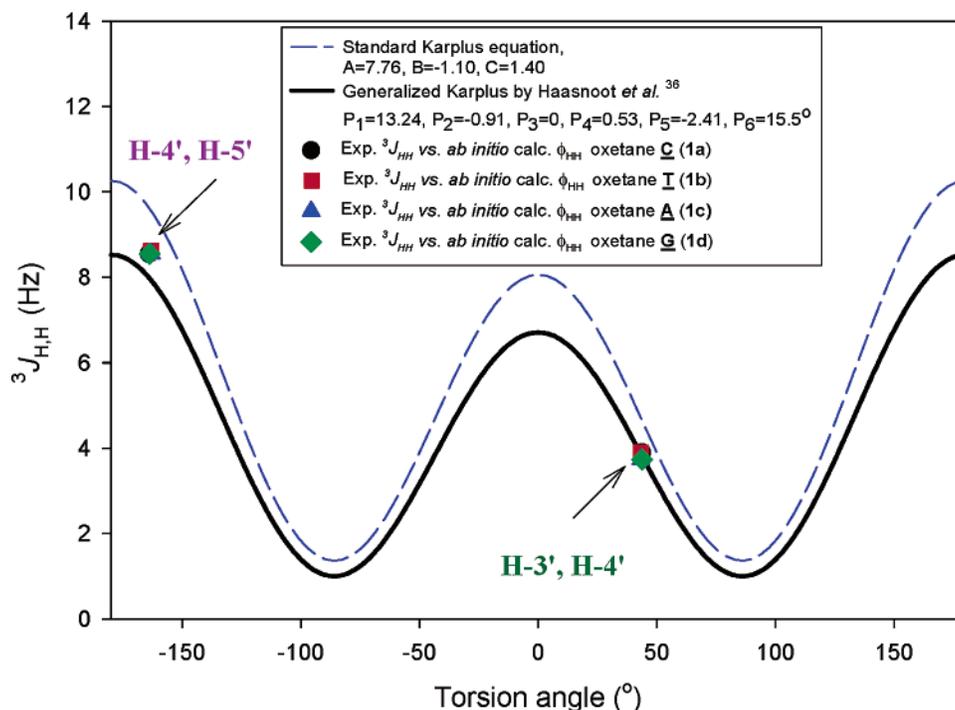
Figure 11. Empirical standard and generalized Karplus dependencies compared to the experimental $^3J_{H,H}$ constants (Hz) (see Table S1 in Supporting Information) for the H-3′, H-4′ and H-4′, H-5′ proton−proton interactions in the oxetane-modified nucleosides plotted against the values of the H3′−C3′−C4′−H4′ and H4′−C4′−C5′−H5′ torsions from the 6-31G* ab initio calculated molecular structures of the oxetane-*C* (**1a**), -*T* (**1b**), -*A* (**1c**), and -*G* (**1d**) nucleosides.

Table 4. Conformational Parameters of the Sugar Moiety of the Oxetane-*C* (**1A**), -*T* (**1b**), -*A* (**1c**), and -*G* (**1d**) Nucleosides Obtained (a) from the ab Initio 6-31G* Hartree−Fock Optimized by Gaussian98[45] Molecular Geometries and (b) from Unrestrained 0.5 ns MD Simulation by Amber 7[46] Averaged in 0.1−0.5 ns Time Interval of the Respective Simulations (shown in parentheses in italics)

sugar conformational parameters	oxetane-*C* (1a)	oxetane-*T* (1b)	oxetane-*A* (1c)	oxetane-*G* (1d)
ν_0: C5′−O5′−C2′−C3′	−15.20° *(−9.7 ± 8.5°)*	−14.30° *(−10.5 ± 9.1°)*	−12.91° *(−7.1 ± 7.8°)*	−14.72° *(−9.3 ± 9.2°)*
ν_1: O5′−C2′−C3′−C4′	−8.57° *(−10.7 ± 5.9°)*	−8.89° *(−10.2 ± 6.2°)*	−9.96° *(−13.6 ± 5.9°)*	−8.82° *(−10.6 ± 6.5°)*
ν_2: C2′−C3′−C4′−C5′	26.34° *(25.0 ± 6.7°)*	26.03° *(24.9 ± 7.5°)*	26.45° *(27.0 ± 5.9°)*	26.49° *(24.5 ± 7.8°)*
ν_3: C3′−C4′−C5′−O5′	−35.76° *(−32.0 ± 9.5°)*	−34.88° *(−32.4 ± 10.7°)*	−34.50° *(−32.8 ± 7.9°)*	−35.55° *(−31.4 ± 10.9°)*
ν_4: C4′−C5′−O5′−C2′	32.66° *(26.7 ± 10.5°)*	31.52° *(27.5 ± 11.6°)*	30.37° *(25.3 ± 8.9°)*	32.11° *(25.8 ± 11.7°)*
phase angle *P*	42.79° *(35.3 ± 18.2°)*	41.87° *(36.6 ± 20.7°)*	39.80° *(30.6 ± 15.3°)*	42.06° *(35.7 ± 20.9°)*
puckering amplitude	36.55° *(32.3 ± 8.7°)*	35.60° *(32.9 ± 9.5°)*	35.07° *(32.7 ± 6.8°)*	36.27° *(31.7 ± 9.7°)*

to that of the native AON/RNA hybrids. The DPPZ group offers excellent 3′-exonuclease protection and augmented stabilities in the Human serum. However, the vulnerability of the oxetane-*A* and *G* modified AONs toward endonucleases might be a drawback. Since we have not checked their tolerance toward cellular endonucleases other than DNase 1, it is not possible to comment at this time on their potential nuclease resistance in the cellular systems, although oxetane-*C* modified AONs were found to be adequately stable in K562 human leukemia cells.[26] It is also worth to mention that, there are reports existing in the literature which show the importance of the modifications at the pyrimidine sites in an AON rather than at purines to achieve endonuclease resistance.[21c,d] Further biological tests are in progress to examine the potential target down-regulation by the oxetane-*A* and -*G* modified AONs in cellular systems.

Conclusions

(1) Oxetane-*A* and -*G* phosphoramidites were synthesized and incorporated into 20mer AONs and targeted to 20mer RNA, and their antisense properties have been evaluated in vitro.

(2) The molecular structures of the oxetane-*C*, *T*, *A*, and *G* monomer units have been studied by means of the high-field

^{1}H NMR and theoretical ab initio and MD simulations. The combined experimental and theoretical studies have demonstrated that the oxetane-fused furanose ring is indeed locked in the typical *North-East*-type conformation with the pseudorotational phase angle (*P*) and puckering amplitude (ϕ_m) for the ab initio optimized geometries (6-31G* HF) varying from 39.8° < *P* < 42.8°, 35.1° < ϕ_m < 36.6° for all four oxetane-modified nucleosides. The last 100 picoseconds (ps) of 0.5 nanosecond (ns) MD simulation starting from the respective ab initio geometries have shown for the oxetane-modified sugars accessible conformational range of *P* and ϕ_m to be 16° < *P* < 56°, 23° < ϕ_m < 41°.

(3) Oxetane-*A* and -*G* modified AONs showed their target affinity with complementary RNA, and the thermodynamic parameters to be identical or very close to the native AON/RNA duplex. However, the oxetane-*C* and oxetane-*T* modified duplexes showed large enthalpic destabilization and slight entropic stabilization compared to that of the native hybrid duplex. The large drop in enthalpy amounts to 32 to 37 kJ/mol drop in the free energy.

(4) The global helical structure of all the oxetane modified AON/RNA hybrids, as revealed by the CD spectra, was very

similar to the native AON/RNA duplex showing that the CD failed to detect the local conformational perturbations brought about by the *North-East* conformationally constrained oxetane modifications.

(5) All of the oxetane-*A* and oxetane-*G* modified AON/RNA hybrid duplexes were found to be good substrates for the *E. coli* RNase H1. In the oxetane-*A* and-*G* modified AON/RNA hybrids, except for one case, a region of 5 nucleotides in the RNA strand in the 3′-end direction from the site opposite to the oxetane modification, was found to be insensitive toward RNase H cleavage presumably owing to the local structural perturbations brought about by the conformationally constrained modifications.

(6) Michaelis−Menten kinetic analysis showed that triple oxetane-*A* modified AON/RNA duplex has V_{max} slightly lower than those of the native and the triple oxetane-*C* modified AON/RNA hybrids. However, the K_m is very close to the native yielding a k_{cat}/K_m close to it. The triple *G* modified AON/RNA duplex showed low K_m and low V_{max} compared to the native counterpart resulting in a k_{cat}/K_m value being half of that of the native AON/RNA hybrid.

(7) The conjugation of nontoxic DPPZ group at the 3′-end of the oxetane-*A* and -*G* modified AONs increases the T_m of the respective AON/RNA duplexes only by 1−2 °C in comparison with their unconjugated counterparts. However, the DPPZ conjugation has helped the AONs to achieve substantial stability against exonuclease ($t_{1/2}$ more than 24 h) and nucleases in human serum ($t_{1/2}$ more than 9 h).

(8) Modification of AONs with the oxetane-*A* and -*G* units failed to offer resistance toward DNase 1 endonuclease degradation in comparison with the oxetane-*C* modified AONs. Thus, DNase 1 appeared to have varying tolerance toward the oxetane-purine and oxetane-pyrimidine nucleotides.

(9) This study unravels the pros and cons of the AONs modified with the oxetane-purine and oxetane-pyrimidine nucleosides and provides valuable information regarding the optimal design of AONs having completely natural phosphodiester backbone for the therapeutic applications.

Experimental Section

Comparative ^{13}C chemical shifts in ppm (δ scale) of the oxetane nucleosides **1a** (*C*), **1b** (*T*), **1c** (*A*), and **1d** (*G*) are shown in Table S2 in Supporting Information.

2-*O*-Methyl-3,4-*O*-isopropylidine-6-*O*-(4-toluoyl)-D-psicofuranose (15). The sugar **14** (9.5 g, 25 mmol) was treated with 0.4 M methanolic HCl (125 mL) overnight. The reaction mixture was cooled, subsequently neutralized with triethylamine, and evaporated. The crude mixture was partitioned between CH$_2$Cl$_2$ and water. The aqueous layer was washed three times with CH$_2$Cl$_2$ and the combined organic layer was dried over MgSO$_4$, filtered, and evaporated. Column chromatography of the residue afforded **15** (5.2 g, 15 mmol, 60%). R_f = 0.5 (CH$_2$Cl$_2$/MeOH 97:3 v/v). ^{1}H NMR (270 MHz, CDCl$_3$): 7.96 (d, 2H, J = 8.29, 4-toluoyl), 7.24 (d, 2H, 4-toluoyl), 4.82 (dd, 1H, $J_{H-3, H-4}$ = 6.06 Hz, $J_{H-4, H-5}$ = 1.2 Hz, H-4), 4.66 (d, H-3), 4.55−4.50 (m, 1H, J_{gem} = 7.2 Hz, $J_{H-5, H-6}$ = 1 Hz, H-6), 4.42−4.30 (m, 2H, H-5, H-6′), 3.84 (Abq, J_{gem} = 9.2 Hz, 2H, H-1, H-1′), 3.29 (s, 3H, OMe), 2.4 (3H, 4-toluoyl), 1.53 (s, 3H, O-acetyl), 1.35 (s, 3H, O-acetyl). ^{13}C NMR (67.9 MHz, CDCl$_3$): 166 (C=O, 4-toluoyl), 143.7, 129.5, 128.9, 126.7 (4-toluoyl), 112.9 (*C*-Me$_2$), 110.1 (C-2), 85.3 (C-3), 84.0 (C-6), 82.0 (C-4), 64.6 (C-5), 58.3 (C-1), 48.4(OCH$_3$), 26.0, 24.7 (CH$_3$, isopropyl), 21.4 (CH$_3$, 4-toluoyl). FAB−HRMS: [MH]$^+$ 353.1624; calcd 353.1602.

1-*O*-Methanesulfonyl-2-*O*-methyl-3,4-*O*-acetyl-6-*O*-(4-toluoyl)-D-psicofuranose (16). Compound **15** (5.2 g, 15 mmol) was coevaporated

with pyridine three times and dissolved in 105 mL of the same solvent. The mixture was cooled in an ice bath and methanesulfonyl chloride (3.2 mL, 41.3 mmol) was added dropwise to the mixture and the stirring was continued for 15 min at the same temperature. The reaction was kept at 4 °C for 12 h, poured into cold saturated NaHCO$_3$ solution and extracted with CH$_2$Cl$_2$. The organic phase was washed with brine, dried over MgSO$_4$, filtered, evaporated, and coevaporated with toluene and treated with 60 mL of 90% CF$_3$COOH in water for 25 min at r.t. The reaction mixture was evaporated, coevaporated three times with toluene and three times with dry pyridine. The residue was dissolved in 75 mL of dry pyridine, acetic anhydride (8.6 mL, 90 mmol) was added and stirred at room temperature for 3 h. The reaction mixture was poured into saturated NaHCO$_3$ solution and extracted with CH$_2$Cl$_2$. The organic phase was washed with brine, dried over MgSO$_4$, filtered, evaporated, and coevaporated with toluene. Column chromatography afforded **16** (5.3 g, 11.3 mmol, 75% after three steps). R_f = 0.6 (MeOH/CH$_2$Cl$_2$ 97:3 v/v). ^{1}H NMR (270 MHz, CDCl$_3$): 7.95 (d, d, J = 8.2 Hz, 2H, 4-toluoyl), 7.25 (d, 2H, 4-toluoyl), 5.65 (dd, $J_{H-3, H-4}$ = 4.6 Hz, $J_{H-4, H-5}$ = 7.9 Hz, 1H, H-4), 5.44 (d, 1H, H-3), 4.58 (dd, J_{gem} = 11.8 Hz, $J_{H-5, H-6}$ = 3.3 Hz, 1H, H-6), 4.51−4.45 (m, 1H, H-5), 4.38 (Abq, J_{gem} = 11.5 Hz, 2H, H-1, H-1′), 4.35 (dd, $J_{H-5, H-6}$ = 3.3 Hz, 1H, H-6′), 3.29 (s, 3H, OCH$_3$), 3.05 (s, 3H, mesyl), 2.42 (s, 3H, 4-toluoyl), 2.16 (s, 3H, O-acetyl), 2.01 (s, 3H, O-acetyl). ^{13}C NMR (67.9 MHz, CDCl$_3$): 169.3, 169 (C=O, acetyl), 166 (C=O, 4-toluoyl), 144.0, 129.6, 129.1, 126.7 (4-toluoyl), 106.2 (C-2), 79.0 (C-5), 73.6 (C-3), 71.0 (C-4), 63.5 (C-6), 61.3 (C-1), 48.9 (OCH$_3$), 38.0 (CH$_3$, mesyl), 21.6 (CH$_3$, 4-toluoyl), 20.4, 20.3 (CH$_3$, O-acetyl). FAB−HRMS: [MH]$^+$ 475.1263; calcd 475.1276.

9-[1′-*O*-Methanesulfonyl-3′,4′-*O*-acetyl-6′-*O*-(4-toluoyl)-β-D-psicofuranosyl]-*N*^{6}-benzoyladenine (18a). The sugar **16** (10 g, 21 mmol) was dissolved in 70 mL of dichloromethane (DCM) and treated with HBr/acetic acid solution (70 mL) for 12 h. The mixture was poured into ice cold water and extracted three times with DCM. The combined organic phase was washed once with saturated NaHCO$_3$ solution followed by saturated NaCl solution. Finally, the organic phase was dried over MgSO$_4$, filtered, evaporated, and coevaporated twice with dry toluene. The crude bromosugar was dissolved in dry dichloroethane-CH$_3$CN (6:1; 140 mL) and added to silylated *N*^{6}-benzoyladenine. [Silylation of *N*^{6}-benzoyladenine: Nucleobase (7.2 g, 30 mmol) was suspended in hexamethyldisilazane (100 mL) and trimethylchlorosilane (6 mL) was added. The reaction mixture was stirred at 120 °C under argon atmosphere for 12 h. The volatile material was evaporated, coevaporated with dry toluene and the residue was dried for 20 min using an oil pump]. The mixture was cooled in an ice bath and SnCl$_4$ (5.25 mL) was added. After stirring in an ice bath for 10 min, the reaction mixture was heated at 70 °C for 3h and continued stirring overnight at r.t. The reaction mixture was poured into saturated NaHCO$_3$ solution, passed through diatomaceous earth and extracted with CH$_2$Cl$_2$. The combined organic phase was washed with brine, dried over MgSO$_4$, filtered and evaporated. The residue on chromatography furnished **18a** (6.1 g, 8.8 mmol, 42%). R_f = 0.5 (MeOH/CH$_2$Cl$_2$ 96:4 v/v). ^{1}H NMR (270 MHz, CDCl$_3$): 8.85 (br s, 1H, NH), 8.69 (s, 1H, H-2), 8.20 (s, 1H, H-8), 7.99 (d, J = 7.92 Hz, 2H, 4-toluoyl), 7.67−7.52 (m, 5H, benzoyl), 7.01(d, 2H, 4-toluoyl,) 6.53 (d, $J_{H-3′, H-4′}$ = 5.32 Hz, 1H, H-3′), 5.61 (dd, $J_{H-4′, H-5′}$ = 3.96 Hz, 1H, H-4′), 4.97−4.79 (m, $J_{H-1′, H-1″}$ = 11.5, 4H, H-5′, H-1′, H-1″, H-6′), 4.37 (dd, J_{gem} = 12.6 Hz, $J_{H-5′, H-6′}$ = 2.97 Hz, H-6″), 2.84 (s, 3H, CH$_3$, mesyl), 2.28 (s, 6H, CH$_3$, 4-toluoyl, CH$_3$, O-acetyl), 2.16 (s, 3H, CH$_3$, O-acetyl). ^{13}C NMR (67.9 MHz, CDCl$_3$): 169.3, 168.5 (C=O, acetyl), 165.5 (C=O, 4-toluoyl), 164 (C=O, benzoyl), 152.6 (C-6), 150.1 (C-4), 149.4 (C-2), 144.5 (4-toluoyl), 140.7 (C-8), 133.5, 132.7 (benzoyl) 129.7, 129.2, 128.9, 127.6, 125.3 (4-toluoyl, benzoyl), 123.0 (C-5), 94.9 (C-2′), 82.4 (C-5′), 74.8 (C-3′), 71.7 (C-4′), 68.0 (C-1′), 62.8 (C-6′), 37.8 (CH$_3$, mesyl), 21.4 (CH$_3$, 4-toluoyl), 20.3 (CH$_3$, O-acetyl). FAB−HRMS: [MH]$^+$ 682.1767; calcd 682.1819.

9-[1′-*O*-Methanesulfonyl-4′,6′-*O*-(tetraisopropyldisiloxane-1,3-diyl)-β-D-psicofuranosyl]adenine (19a). Compound **18a** (6.1 g, 9 mmol) was treated with methanolic NH$_3$ solution for 48 h at room temperature. The mixture was evaporated, triturated with dichloromethane, coevaporated three times with pyridine and dissolved in 90 mL of the same solvent. The mixture was cooled in an ice bath and 1,3-dichloro-1,1′,3,3′-tetraisopropyldisiloxane (2.88 mL, 9 mmol) was added dropwise. The mixture was stirred at 0 °C for 30 min and at r.t. for 2 h. It was poured into saturated NaHCO$_3$ solution and extracted with CH$_2$Cl$_2$. The organic phase was dried, evaporated and coevaporated with toluene. Column chromatography of the residue afforded compound **19a** (4.1 g, 6.47 mmol, 72%). R_f = 0.6 (CH$_2$Cl$_2$/MeOH 94:6 v/v). ^{1}H NMR (270 MHz, CDCl$_3$): 8.34 (s, 1H, H-2), 8.21(s, 1H, H-8), 5.86 (br s, 2H, NH$_2$), 5.28 (d, J_{gem} = 11.8 Hz, 1H, H-1′), 4.94 (d, 1H, $J_{H-3′, H-4′}$ = 4.4, H-3′), 4.9 (d, 1H, H-1″), 4.41 (dd, $J_{H-3′, H-4′}$ = 4.3 Hz, $J_{H-5′, H-4′}$ = 8.54 Hz, 1H, H-4′), 4.32 (dt, 1H, $J_{H-5′, H-6′}$ = 2.47, H-5′), 4.25–4.03 (ddd, J_{gem} = 13.2 Hz, $J_{H-5′, H-6′}$ = 2.72 Hz, 2H, H-6′, H-6″), 1.07–0.85 (m, 28 H, Si–C*H*(CH$_3$)$_2$ and CH$_3$ from 4-^{i}Pr). ^{13}C NMR (67.9 MHz, CDCl$_3$): 155.5 (C-6), 152.7 (C-2), 148.2 (C-4), 139.4 (C-8), 120.6 (C-5), 94.9 (C-2′), 82.5 (C-5′),75.3 (C-3′), 69.6 (C-4′), 68.8 (C-1′), 60.3 (C-6′), 37.5 (CH$_3$, mesyl), 17.1, 17.0, 16.9, 16.8 (Si-CH(*C*H$_3$)$_2$), 13.3, 12.9, 12.5, 12.4 (Si–*C*H(CH$_3$)$_2$). FAB–HRMS: [MH]$^+$ 618.2427; calcd 618.2449.

9-[1′-3′-*O*-Anhydro-4′,6′-*O*-(tetraisopropyldisiloxane-1,3-diyl)-β-D-psicofuranosyl]adenine (20a). Compound **19a** (3.19 g, 5.2 mmol, 1M solution in THF) was dissolved in THF (100 mL) and cooled in an ice bath. Sodium bis(trimethylsilyl)amide) (10 mL, 10 mmol, 1 M solution in THF) was added in dropwise and the stirring was continued for 2 h. The reaction was quenched by adding saturated NaHCO$_3$ and extracted with excess of ethyl acetate. The combined organic phase was dried, filtered, and evaporated. The residue on column chromatography yielded **20a** (2.2 g, 4.2 mmol, 81%). R_f = 0.5 (ethyl acetate/cyclohexane 93:7 v/v). ^{1}H NMR (270 MHz, CDCl$_3$): 8.28 (s, 1H, H-2), 7.79 (s, 1H, H-8), 5.86 (br s, 2H, NH$_2$), 5.74 (d, $J_{H-3′, H-4′}$ = 3.9 Hz, 1H, H-3′), 5.58 (d, J_{gem} = 7.8 Hz, 1H, H-1′), 5.01 (d, 1H, H-1″), 4.83 (dd, $J_{H-4′, H-5′}$ = 8.5 Hz, H-4′), 4.49 (dt, $J_{H-5′,H-6′}$ = 2.5 Hz, 1H,H-5′), 4.18 (ddd, $J_{H-5′, H-6″}$ = 3 Hz, J_{gem}=13.5, 2H, H-6′,H-6″), 1.12–1.03 (m, 28 H, Si–C*H*(CH$_3$)$_2$ and CH$_3$ from 4-^{i}Pr).^{13}C NMR (67.9 MHz, CDCl$_3$): 155.7 (C-6), 153.4 (C-2), 149.6 (C-4), 137.2 (C-8), 119.4 (C-5), 88.9 (C-3′), 87.8 (C-2′); 81.4 (C-5′), 79.5 (C-1′), 70.6 (C-4′), 59.8 (C-6′), 17.21, 17.15, 17.03, 16.9 (Si-CH(*C*H$_3$)$_2$), 13.3, 12.9, 12.4 (Si–*C*H(CH$_3$)$_2$). FAB–HRMS: [MH]$^+$ 522.2540; calcd 522.2568. A small amount of **20a** was deprotected to get 9-(1′,3′-*O*-anhydro-β-D-psicofuranosyl)adenine (**1c**) and data is shown in Table 3 and Table S2 in the Supporting Information. FAB–HRMS: [MH]$^+$ 280.1040; calcd 280.1046.

9-[1′-3′-*O*-Anhydro-4′,6′-*O*-(tetraisopropyldisiloxane-1,3-diyl)-β-D-psicofuranosyl]-*N*^{6}-(phenoxy-acetyl)-adenine (21a). Compound **20a** (1.8 g, 3.5 mmol) was dissolved in pyridine (25 mL) and phenoxyacetyl chloride (0.64 mL, 4.6 mmol) was added dropwise to the reaction mixture. Stirring was continued for 3 h at r.t. The mixture was poured into sat. NaHCO$_3$ solution extracted with CH$_2$Cl$_2$. Combined organic phase evaporated and coevaporated with toluene. Column chromatography of the residue furnished compound **21a** (1.4 g, 2.1 mmol, 60%). R_f = 0.6 (CH$_2$Cl$_2$/MeOH 94:6 v/v). ^{1}H NMR (270 MHz, CDCl$_3$): 9.5 (br s, 1H, NH), 8.74 (s, 1H, H-2), 8.02 (s, 1H, H-8), 7.37–7.01 (m, 5H, PAC), 5.76 (d, J = 3.9 Hz, 1H, H-3′), 5.59 (d, 1H, J_{gem} = 7.8 Hz, H-1′), 5.03 (d, 2H, J_{gem} = 8.0 Hz, H-1″), 4.92–4.82 (m, $J_{H-4′, H-5′}$ = 3.9 Hz, $J_{H-4′, H-3′}$ = 8.7 Hz, 3 H, H-4′, C*H$_2$* PAC), 4.50 (dt, $J_{H-5′, H-6′}$ = 2.0 Hz, $J_{H-4′, H-5′,}$ = 8.7 Hz, 1H, H-5′), 4.25–4.12 (ddd, J_{gem} = 13.9 Hz, $J_{H-5′, H-6′}$ = 2.4 Hz, $J_{H-5′, H-6″}$ = 2.7 Hz, 2H, H-6′, H-6″), 1.13–1.05 (m, 28 H, Si–C*H*(CH$_3$)$_2$ and CH$_3$ from 4-^{i}Pr). ^{13}C NMR (67.9 MHz, CDCl$_3$): 166.5 (C=O), 156.9 (C-6), 152.9 (C-2), 151.3 (C-4), 148.4, 140.1 (C-8), 129.7, 122.6, 122.3, 114.8 (C-5), 88.7 (C-3′), 87.9 (C-2′); 81.7 (C-5′), 79.3 (C-1′), 70.5 (C-4′), 68.0 (*C*H$_2$, PAC), 59.7 (C-6′), 17.2, 17.0, 16.9, 16.8 (Si-CH(*C*H$_3$)$_2$), 13.3, 12.9, 12.4 (Si–CH(*C*H$_3$)$_2$). FAB–HRMS: [MH]$^+$ 656.2949; calcd 656.2936.

9-[1′-3′-*O*-Anhydro-6′-*O*-(4,4′-dimethoxytrityl)-β-D-psicofuranosyl]-*N*^{6}-(phenoxyacetyl)-adenine (22a). Compound **21a** (1.7 g, 2.7 mmol) was dissolved in THF (27 mL) and treated with 1.0 M tetra-*n*-butylammonium fluoride in THF (2.7 mL) for 4 min at room temperature. The mixture was evaporated and coevaporated three times with pyridine. It was then dissolved in pyridine (22 mL) and 4,4′-dimethoxytrityl chloride (2 g, 5.94 mmol) was added, and the mixture was stirred at room-temperature overnight. Saturated NaHCO$_3$ solution was added and extracted with CH$_2$Cl$_2$. The organic phase was washed with brine, dried over MgSO$_4$, filtered, evaporated, and coevaporated with toluene. The residue on column chromatography afforded **22a** (1.54 g, 2.1 mmol, 80% in two steps). R_f = 0.4 (ethyl acetate/cyclohexane 93:7 v/v). ^{1}H NMR (270 MHz, CDCl$_3$): 8.80 (s, 1H, H-2), 8.08 (s, 1H, H-8), 7.40–7.01 (m, 14H, DMTr & PAC), 6.79–6.75 (m, 4H, DMTr), 5.79 (d, $J_{H-3′, H-4′}$ = 4.33 Hz, 1H, H-3′), 5.65 (d, J_{gem} = 7.92 Hz, 1H, H-1′), 4.978 (d, 1H, H-1″), 4.87 (s, 1H, CH$_2$, PAC), 4.52 (dd, $J_{H-4′, H-5′}$ = 8.3 Hz, 1H, H-4′), 4.47–4.43 (m, 1H, H-5′), 3.76 (s, OCH$_3$, DMTr), 3.58 (dd, J_{gem} = 10.76 Hz, $J_{H-5′, H-6′}$ = 2.6 Hz, H-6′), 2.98 (dd, $J_{H-5′, H-6″}$ = 2.7 Hz, 1H, H-6″). ^{13}C NMR (67.9 MHz, CDCl$_3$): 166.5 (C=O), 158.5, 157 (DMTr), 152.9 (C-2), 151.2 (C-4), 148.4 (C-6), 144.5 (DMTr), 140.3 (C-8), 135.5, 130, 129.9, 129.8, 128.9, 128.1, 127.9, 127.7, 126.8, 125.2, 122.8, 122.4 (DMTr & PAC), 114.9 (C-5), 113.1 (DMTr), 88.6 (C-3′), 86.3 (C-2′), 84.0 (C-5′), 79.7 (C-1′), 71.5 (C-4′), 68.1 (*C*H$_2$, PAC), 62.5 (C-6′), 55.1 (O*C*H$_3$, DMTr). FAB–HRMS: [MH]$^+$ 716.2784; calcd 716.2720.

9-{1′,3′-*O*-Anhydro-4′-*O*-[2-cyanoethoxy(diisopropylamino)-phosphino]-6′-*O*-(4,4′-di-methoxytrityl)-β-D-psicofuranosyl}-*N*^{6}-(phenoxyacetyl)-adenine (23a). To a stirred solution of **22a** (763 mg, 1.07 mmol) in 7 mL of CH$_2$Cl$_2$, 2-cyanoethoxy-bis(*N*,*N*-diisopropylamino) phosphine (0.62 mL, 1.6 mmol) was added followed by *N*,*N*-diisopropylammonium tetrazolide (92 mg, 0.54 mmol) and left for stirring overnight. The reaction mixture was diluted with of ethyl acetate, poured into saturated NaHCO$_3$ solution and extracted. The organic layer was washed with saturated brine solution, dried over MgSO$_4$, filtered, and evaporated. The residue on chromatography (40–60% ethyl acetate, cyclohexane + 2% Et$_3$N) furnished **23a** (640 mg, 0.7 mmol, 65%). R_f = 0.6 (ethyl acetate/cyclohexane 93:7 v/v). The compound was dissolved in CH$_2$Cl$_2$ (2 mL) and precipitated from hexane at −40 °C. ^{31}P NMR (109.4 MHz, CDCl$_3$): 151.39; 150.40. FAB–HRMS: [MH]$^+$ 916.3730; calcd 916.3799.

9-[1′-*O*-Methanesulfonyl-3′,4′-*O*-acetyl-6′-*O*-(4-toluoyl)-β-D-psico-furanosyl]-*N*^{2}-acetylguanine (18b). The sugar **16** (4.7 g, 10 mmol) was brominated using the same procedure as used for **18a**. After being kept on an oil pump for 30 min, the crude bromosugar was dissolved in dry (CH$_2$)$_2$Cl$_2$ (60 mL) and added to silylated *N*^{2}-acetyl-*O*^{6}-diphenylcarbamyguanine. [The silylation was carried out by heating *N*^{2}-acetyl-*O*^{6}-diphenyl carbamyguanine (5.8 g, 15 mmol) with *N*,*O*-bis(trimethylsilyl)acetamide (30 mL) in (CH$_2$)$_2$Cl$_2$ (75 mL) at 80 °C for 30 min. The mixture was evaporated, coevaporated with dry toluene and dried on an oil pump for 20 min.] The mixture was cooled in an ice bath and SnCl$_4$ (2.5 mL) was added. After being stirred in an ice bath for 20 min. the reaction mixture was heated at 70 °C for 3 h and continued stirring at r.t. overnight. The reaction mixture was poured into saturated NaHCO$_3$ solution and passed through diatomaceous earth. It was extracted with CH$_2$Cl$_2$ and the combined organic phase was washed with brine, dried over MgSO$_4$, filtered, and evaporated. The residue on chromatography afforded DPC protected nucleoside, which was then treated with 90% triflouroacetic acid in water for 30 min to remove the DPC group. The reaction mixture was evaporated, coevaporated with toluene and a quick column furnished **18b** (1.6 g, 2.5 mmol, 25%). R_f = 0.5 (CH$_2$Cl$_2$/MeOH 90:10 v/v). ^{1}H NMR (270 MHz, CDCl$_3$): 12.01 (s, 1H, NH), 9.59 (s, 1H, NH), 7.98 (s, 1H, H-8), 7.67 (d, J = 8.16 Hz, 2H, 4-toluoyl), 7.20 (d, 4-toluoyl), 6.56 (d, J = 4.82 Hz, 1H, H-3′), 5.52 (dd, $J_{H-3′, H-4′}$ = 7.42 Hz, $J_{H-4′, H-5′}$ = 2.72 Hz, 1H, H-4′), 4.86 (d, J_{gem} = 11.38 Hz 1H, H-1′), 4.7–4.64 (m, 3H, H-5′, H-1′, H-6′), 4.53 (dd, J_{gem} = 12.8 Hz, $J_{H-6′, H-5′}$ = 4.33 Hz, 1H, H-6′),

2.87 (s, 3H, CH₃, mesyl), 2.38 (s, 3H, CH₃, 4-toluoyl), 2.27(s, 3H, CH₃, *O*-acetyl), 2.2 (s, 3H, CH₃, *O*-acetyl), 2.05 (s, 3H, CH₃, *N*-acetyl). ¹³C NMR(67.9 MHz, CDCl₃): 172.0(C=O, C-6), 169.1 (C=O, N-2 acetyl), 168.8 (C=O, 4-toluoyl), 165.8, 155.2 (C-6), 147.0 (C-2), 146.8 (C-4), 144.4 (4-toluoyl), 136.8 (C-8), 129.2, 129.0, 125.6 (4-toluoyl), 122.0 (C-5), 94.4 (C-2′); 80.0 (C-5′), 73.3 (C-3′), 69.7 (C-4′), 67.0 (C-1′), 61.6 (C-6′), 37.7 (CH₃, mesyl), 24.1 (CH₃, O-acetyl), 21.4 (CH₃, 4-toluoyl), 20.2 (CH₃, O-acetyl) 20.1 (CH₃, N-acetyl). FAB−HRMS: [MH]⁺ 636.1667; calcd 636.1564.

9-[1′-*O*-Methanesulfonyl-4′,6′-*O*-(tetraisopropyldisiloxane-1,3-diyl)-β-D-psicofuranosyl]guanine (19b). Compound **18b** (2.2 g, 3.5 mmol) was deprotected and reated with 1,3-dichloro-1,1′,3,3′-tetraisopropyldisiloxane (1.1 mL, 3.5 mmol) using the same procedure described for compound **19a**. After workup and chromatography afforded **19b** (1.4 g, 2.2 mmol, 63% yield). R_f = 0.6 (CH₂Cl₂/MeOH 90:10 v/v). ¹H NMR (270 MHz, CD₃OD): 8.03 (s, 1H, H-8), 5.29 (d, J_{gem} = 11.75 Hz, 1H, H-1′), 5.04 (d, $J_{H-3′, H-4′}$ = 3.34 Hz, 1H, H-3′), 4.79 (d, 1H, J_{gem} = 11.75 Hz, H-1′′), 4.45−4.34 (m, 3H, H-4′, H-5′, H-6′), 4.13 (dd, J_{gem} = 15.96, $J_{H-5′, H-6′}$ = 2.60 Hz, 1H, H-6′′), 3.03 (s, 1H, mesyl), 1.2−1.02 (m, 28 H, Si−C*H*(CH₃)₂ and CH₃ from 4-*i*Pr). ¹³C NMR (67.9 MHz, CD₃OD): 159.7 (C-6), 155.2 (C-2), 151.5 (C-4), 138.3 (C-8), 119.2 (C-5), 96.6 (C-2′), 83.6 (C-5′), 76.3 (C-3′), 70.9 (C-1′), 70.7 (C-4′), 61.1 (C-6′), 37.5 (OMs), 18.2, 18.1, 17.7, 17.7 (Si-C*H*(CH₃)₂), 14.9, 14.5, 14.2, 14.1 (Si−CH(C*H*₃)₂). FAB−HRMS: [MH]⁺ 634.2432; calcd 634.2401.

9-[1′-3′-*O*-Anhydro-4′,6′-*O*-(tetraisopropyldisiloxane-1,3-diyl)-β-D-psicofuranosyl]guanine (20b). Compound **19b** (1.4 g, 2.2 mmol) was cyclized using the procedure as described for **20a**. After work up and chromatography of the residue furnished **20b** (990 mg, 1.8 mmol, 83%) R_f = 0.6 (CH₂Cl₂/MeOH 88:12 v/v). ¹H NMR (270 MHz, DMSO-d_6): 7.85 (s, 1H, H-8), 6.32 (s, 2H, NH₂), 5.70 (d, $J_{H-3′, H-4′}$ = 3.9 Hz, 1H, H-3′), 5.39 (d, J_{gem} = 8.3 Hz, 1H, H-1′), 4.95 (d, 1H, H-1′′), 4.58 (dd, $J_{H-4′, H-5′}$ = 8.3 Hz 1H, H-4′), 4.44 (dt, $J_{H-5′, H-6′}$ = 3.0 Hz, 1H, H-5′), 4.13 (d, 2H, H-6′, H-6′′), 1.18−1.09 (m, 28 H, Si−C*H*(CH₃)₂ and CH₃ from 4-*i*Pr). ¹³C NMR (67.9 MHz, DMSO-D6): 156.8 (C-6), 153.8 (C-2), 151 (C-4), 135 (C-8), 116.9 (C-5), 87.6 (C-3′), 87.4 (C-2′), 80.7 (C-5′), 79.0 (C-1′), 71.8 (C-4′), 60.7 (C-6′), 17.3, 17.2, 17.1, 16.9 (Si-C*H*(CH₃)₂), 12.8, 12.6, 12.3, 12.2 (Si−CH(C*H*₃)₂). FAB−HRMS: [MH]⁺ 538.2525; calcd 538.2517. A small amount of **20b** was deprotected to get 9-(1′,3′-*O*-anhydro-β-D-psicofuranosyl)guanine (**1d**) and the data are shown in Table 3 and in Table S2 in Supporting Information. FAB−HRMS: [MH]⁺ 296.0990; calcd 296.0997.

9-[1′-3′-*O*-Anhydro-4′,6′-*O*-bis (tetraisopropyldisiloxane-1,3-diyl)-β-D-psicofuranosyl]-*N²*-(*N,N*-dimethylamino methylene)guanine (21b). To a stirred solution of compound **20b** (733 mg, 1.4 mmol) in dry MeOH (13 mL), *N,N*-dimethylformamide dimethylacetal (0.9 mL, 6.8 mmol) was added and allowed to stir at r.t. overnight. The mixture was evaporated and coevaporated with toluene. Column chromatography of the residue furnished compound **21b** (757 mg, 1.27 mmol, 91%). R_f = 0.5 (CH₂Cl₂/MeOH 90:10 v/v). ¹H NMR (270 MHz, CDCl₃): 8.5 (s, 1H, N=C*H*), 7.59 (s, 1H, H-8), 5.67 (d, J_{gem} = 9 Hz, 1H, H-1′), 5.64 (d, $J_{H-3′, H-4′}$ = 4.3 Hz, 1H, H-3′), 4.93 (d, 1H, H-1′′), 4.44 (dt, $J_{H-4′, H-5′}$ = 8.5 Hz, 1H, H-5′), 4.38 (dd, 1H, H-4′), 4.23−4.10 (ddd, J_{gem} = 13.0 Hz, $J_{H-5′, H-6′}$ = 2.5 Hz, $J_{H-5′, H-6′′}$ = 2.4 Hz, 2H, H-6′, H-6′′), 3.19, 3.13 (2s, 6H, N(CH₃)₂), 1.10−1.04 (m, 28 H, Si−C*H*(CH₃)₂ and CH₃ from 4-*i*Pr). ¹³C NMR (67.9 MHz, CDCl₃): 157.7 (N=C*H*), 157.5 (C-2), 156.7 (C-6), 149.8 (C-4), 135.1 (C-8), 120.9 (C-5), 88.9 (C-3′), 88.6 (C-2′); 81.0 (C-5′), 80.2 (C-1′), 71.5 (C-4′), 60.0 (C-6′), 41.3, 35.2 (N(CH₃)₂), 17.22, 17.13, 17.0, 16.9, (Si-C*H*(CH₃)₂), 13.5, 12.9, 12.6 (Si−CH(C*H*₃)₂). FAB−HRMS: [MH]⁺ 593.2951; calcd 593.2939.

9-[1′-3′-*O*-Anhydro-6′-*O*-(4,4′-dimethoxytrityl)-β-D-psicofuranosyl]-*N²*-(*N,N*-(dimethylamino)-methylene)-guanine (22b). From compound **21b** (680 mg, 1.2 mmol), the TIPS group was removed and treated with 4,4′-dimethoxytrityl chloride (780 mg, 2.3 mmol) using the method described for compound **22a** to afford **22b** (614 mg, 1 mmol, 83% in two steps). R_f = 0.5 (CH₂Cl₂/MeOH 90:10 v/v). ¹H NMR

(270 MHz, CDCl₃): 8.42 (s, 1H, N=C*H*), 7.63 (s, 1H, H-8), 7.42−7.17 (m, 9H, DMTr), 6.79−6.75 (m, 4H, DMTr), 5.71 (d, $J_{H-3′, H-4′}$ = 3.6 Hz, 1H, H-3′), 5.54 (d, J_{gem} = 7.7 Hz, 1H, H-1′), 4.94 (d, 1H, H-1′′), 4.45−4.37 (m, 2H, H-4′, H-5′), 3.77 (s, OCH₃, DMTr); 3.58−3.45 (ddd, J_{gem} = 11 Hz, $J_{H-5′, H-6′}$ = 2.6 Hz, $J_{H-5′, H-6′′}$ = 2.7 Hz, 2H, H-6′, H-6′′), 3.05, 3.01 (2s, 6H, −N(CH₃)₂). ¹³C NMR (67.9 MHz, CDCl₃): 158.4 (DMTr), 157.9 (N=CH), 157.5, 156.7 (C-6), 149.8 (C-4), 144.4, 135.59, 135.54 (DMTr), 135.1 (C-8), 129.9, 128.1, 127.7, 126.7 (DMTr), 120.7 (C-5), 113.0 (DMTr), 88.6 (C-3′), 86.2 (C-2′), 83.1 (C-5′), 79.9 (C-1′), 71.6 (C-4′), 62.4 (C-6′), 55.1 (OCH₃, DMTr), 41.3, 35.1 (N(C*H*₃)₂). FAB−HRMS: [MH]⁺ 653.2749; calcd 653.2724.

9-{1′,3′-*O*-Anhydro-4′-*O*-[2-cyanoethoxy(diisopropylamino)-phosphino]-6′-*O*-(4,4′-di-methoxytrityl)-β-D-psicofuranosyl}-*N²*-(*N,N*-dimethylaminomethylene)-guanine (23b). Compound **22b** (392 mg, 0.6 mmol) was converted to the corresponding phosphoramidite using the conditions described for **23a**. Workup and chromatography (80−100% CH₂Cl₂, cyclohexane + 2% Et₃N) furnished **23b** (341 mg, 0.44 mmol, 73%). R_f = 0.6 (CH₂Cl₂/MeOH 94:6 v/v). The compound was dissolved in CH₂Cl₂ (2 mL) and precipitated from hexane at −40 °C. ³¹P NMR (109.4 MHz, CDCl₃): 152.12; 149.89. FAB−HRMS: [MH]⁺ 858.3817; calcd 853.3802.

Synthesis, Deprotection and Purification of Oligonucleotides. All oligonucleotides were synthesized using an automated DNA/RNA synthesizer by Applied Biosystems, model 392. For modified AONs containing oxetane-*A*, -*G*, -*C*, and -*T* units, fast deprotecting phosphoramidites (nucleobases were protected using the following groups: Ac for C, *i*Pr−PAC for G, and PAC for A) were used. The protected AONs were deprotected at room temperature by the treatment of aqueous NH₃ for 24 h. For the 3′-DPPZ conjugated AONs, a CPG support containing DPPZ was used.[25] All AONs and the target RNA were purified by 20% polyacrylamide/7M urea) PAGE, extracted with 0.3 M NaOAc, desalted with C18-reverse phase catridges and their purity (greater than 95%) was confirmed by PAGE. MALDI-MS analysis: AON (**2**) [MH]⁻ = 6128.37; calcd 6127.01; AON (**3**) [MH]⁻ = 6127.18; calcd = 6127.01; AON (**4**) [MH]⁻ = 6127.86; calcd = 6127.01; AON (**5**) [MH]⁻ = 6129.72; calcd 6127.01; AON (**6**) [MH]⁻ = 6127.44; calcd = 6127.01; AON (**7**) [MH]⁻ = 6211.51; calcd = 6211.04; AON (**8**) [MH]⁻ = 6735.68; calcd = 6736.48; AON (**9**) [MH]⁻ = 6737.88; calcd = 6736.48; AON (**12**) [MH]⁻ = 6178.81; calcd = 6178.02.

UV Melting Experiments. Determination of the T_m of the AON/RNA hybrids was carried out in the following buffer: 57 mM Tris-HCl (pH 7.5), 57 mM KCl, 1 mM MgCl₂. Absorbance was monitored at 260 nm in the temperature range from 20 °C to 90 °C using UV spectrophotometer equipped with Peltier temperature programmer with the heating rate of 1 °C per minute. Prior to measurements, the samples (1 μM of AON and 1 μM RNA mixture) were preannealed by heating to 90 °C for 5 min followed by slow cooling to 4 °C and 30 min equilibration at this temperature.

Thermodynamic Calculations from the UV Experiments. The thermodynamic parameters characterizing the helix-to-coil transition for the DNA/RNA hybrids were obtained from T_m measurements over the concentration range from 0.6 to 16 μM (total strand concentration). Values of $1/T_m$ were plotted versus $\ln(C_T/4)$ and $\Delta H°$ and $\Delta S°$ parameters were calculated from slope and intercept of fitted line: $1/T_m = (R/\Delta H°)\ln(C_T/S) + \Delta S°/\Delta H°$, where S reflects the sequence symmetry of the self ($S = 1$) or nonself-complementary strands ($S = 4$).

CD Experiments. CD spectra were recorded from 300 to 200 nm in 0.2 cm path length cuvettes. Spectra were obtained with a AON/RNA duplex concentration of 5 μM in 57 mM Tris-HCl (pH 7.5), 57 mM KCl, 1 mM MgCl₂. All the spectra were measured at 5 °C and each spectrum is an average of 5 experiments from which CD value of the buffer was subtracted.

Theoretical Calculations. The structural parameters of the oxetane-modified nucleosides and conformational hyperspace available for the compounds have been determined by the ab initio geometry optimizations followed by the 0.5 ns molecular dynamics simulations. The

geometry optimizations of the oxetane-modified nucleosides have been carried out by the Gaussian 98 program package[45] at the Hartree–Fock level using 6-31G* basis set. The atomic charges and optimized geometries of the oxetane-C (**1a**), -T (**1b**), -A (**1c**), and -G (**1d**) were then used for the Amber force field parameters employed in the MD simulations. The protocol of this MD simulations is based on Cheathan–Kollman's[47] procedure employing modified version of Amber 1994 force field as it is implemented in Amber 7 program package.[46] The TIP3P water model was used to introduce explicit solvent molecules in the MD calculations. Periodic boxes containing 1048, 1125, 1084, and 1122 water molecules were created around the oxetane-C (**1a**), -T (**1b**), -A (**1c**), and -G (**1d**), respectively, extending 12.0 Å from these molecules in all three dimensions.

[32]P Labeling of Oligonucleotides. The oligoribonucleotide, oligodeoxyribonucleotides were 5′-end labeled with ^{32}P using T4 polynucleotide kinase, [γ-^{32}P]ATP and standard procedure.[48] Labeled AONs and RNA were purified by 20% denaturing PAGE and specific activities were measured using Beckman LS 3801 counter.

Kinetics of RNase H Hydrolysis. (A) Calibration of RNase H Concentration Based on its Cleavage Activity. The source of RNase H1 (obtained from Amersham Bioscience) was *Escherichia coli* containing clone of RNase H gene. The solutions of 20mer AON (**1**)/RNA (**13**) duplex: [AON] = 10^{-6} M, [RNA] = 10^{-7} M (the first control substrate) and 20mer AON (**3**)/RNA (**13**) duplex: [AON] = 10^{-6} M, [RNA] = 10^{-7} M (the second control substrate) in a buffer, containing 20 mM Tris-HCl (pH 8.0), 20 mM KCl, 10 mM MgCl$_2$, 0.1 mM EDTA and 0.1 mM dithiothreitol (DTT) at 21 °C in 30 μL of the total reaction volume have been used as standard substrates to calibrate the amount of RNase H actually used. The percentage of RNA cleavage was monitored by gel electrophoreses as a function of time (1–5 min), with using of 0.08 U of RNase H, to give the initial velocity. *Thus, the initial velocity of the RNase H cleavage reaction, 5.4171×10^{-3} μM/ min (for the first standard substrate control) or 2.0869×10^{-3} μM/ min (for the second standard substrate control) under the above condition corresponds to 0.08 units activity of enzyme in 30 μL of the total reaction mixture.* These are based on 9 independent experiments. Since Michaelis equation suggests that the initial velocity of the reaction linearly depends on the enzyme concentration, therefore, using the initial velocity for the first standard substrate control or the second standard substrate control corresponding to 0.08 units/30 μL concentration of the RNase H, two correlation coefficients were found by dividing the observed experimental initial velocity by the standard initial velocity of 5.4171×10^{-3} or 2.0869×10^{-3} μM/min. Then, the real enzyme concentration as well as the initial velocity in each experiment was corrected using average value of the correlation coefficients of both the standard substrate controls, which were used to calibrate the initial velocity of the RNase H promoted cleavage reaction for each substrate presented in this work.

(B) RNA Concentration Dependent Experiments. ^{32}P-Labeled RNA (0.01 to 0.8 μM, specific activity 50 000 cpm) with AONs (4 μM) were incubated with 0.08 units of RNase H in buffer, containing 20 mM Tris-HCl (pH 8.0), 20 mM KCl, 10 mM MgCl$_2$ and 0.1 mM DTT at 21 °C. Total reaction volume was 30 μL. Prior to the addition of the enzyme reaction components were preannealed in the reaction buffer by heating at 80 °C for 5 min followed by 1.5 h equilibration at 21 °C. After 1–7 min, aliquots (3 μL) were mixed with stop solution (6 μL), containing 0.05 M disodium salt of the ethylenediamine-

tetraacetic acid (EDTA), 0.05% (w/v) bromophenol blue and 0.05% (w/v) xylene cyanol in 95% formamide, and subjected to 20% 7 M urea denaturing gel electrophoresis. The kinetic parameters K_m and V_{max} were obtained from v_0 versus $[S_0]$ plots obeying Michaelis–Menton equation: $v_0 = V_{max} \cdot S_0 / K_m + S_0$. Values of K_m and V_{max} at this method were determined directly from v_0 versus $[S_0]$ plots by using of correlation Program, where correlation equation was: $y = ax/(b + x)$ where $a = V_{max}$ and $b = K_m$. Since the $V_{max} = E_0 \cdot k_{cat}$ (E_0 = initial enzyme concentration), and for all of our RNA concentration dependent kinetics, the E_0 was identical, hence V_{max} is proportional to k_{cat}. In other words, the k_{cat} can be understood by comparing simply the V_{max}.

Exonuclease Degradation Studies. Stability of the AONs toward 3′-exonucleases was tested using snake venom phosphodiesterase from *Crotalus adamanteus*. All reactions were performed at 3 μM DNA concentration (5′-end ^{32}P labeled with specific activity 50 000 cpm) in 56 mM Tris-HCl (pH 7.9) and 4.4 mM MgCl$_2$ at 22 °C. Exonuclease concentration of 35 ng/μL was used for digestion of oligonucleotides. Total reaction volume was 14 μL. Aliquots were taken at 1, 2, 4, and 24 h and quenched by addition of the same volume of 50 mM EDTA in 95% formamide. Reaction progress was monitored by 20% denaturing (7 M urea) PAGE and autoradiography.

Endonuclease Degradation Studies. Stability of AONs toward endonuclease was tested using DNase 1 from bovine pancreas. Reactions were carried out at 0.9 μM DNA concentration (5′-end ^{32}P labeled with specific activity 50 000 cpm) in 100 mM Tris-HCl (pH 7.5) and 10 mM MgCl$_2$ at 37 °C using 20 unit of DNase 1. Total reaction volume was 22 μL. Aliquots were taken at 1, 2, 4, 8 and 12 h and quenched with the same volume of 50 mM EDTA in 95% formamide. They were resolved in 20% polyacrylamide denaturing (7 M urea) gel electrophoresis and visualized by autoradiography.

Stability Studies in Human Serum. AONs (6 μL) at 2 μM concentration (5′-end ^{32}P labeled with specific activity 90 000 cpm) were incubated in 30 μL of human serum (male AB) at 22 °C (total reaction volume was 36 μL). Aliquots (3 μL) were taken at 0, 15 and 30 min, 1, 2 and 9 h, and quenched with 6 μL of solution containing 8 M urea and 50 mM EDTA, resolved in 20% polyacrylamide denaturing (7 M urea) gel electrophoresis and visualized by autoradiography.

Supporting Information Available: (1) General experimental procedures; (2) Figure S1: CD spectra of AON (**1**–**4**, **7**, and **10**)/RNA (**13**) duplexes; (3) Figure S2: PAGE analysis of the DNase 1 degradation of AON (**1**)–(**4**), (**7**), and (**11**); (4) Figure S3: PAGE analysis of the snake venom phosphodiesterase (SVPDE) degradation of AONs (**1**), (**7**), (**12**), (**8**), (**9**) and (**11**); (5) Figure S4: PAGE analysis of the degradation of AONs (**1**), (**7**), (**12**), (**8**), (**9**) and (**11**) in human serum; (6) Table S1: Experimental and calculated vicinal $^3J_{H,H}$ coupling constants; (7) Table S2: Carbon chemical shifts in ppm (δ scale) of the oxetane nucleosides **1a** (*C*), **1b** (*T*), **1c** (*A*), and **1d** (*G*); (8) Figures S4–S16: ^{13}C NMR spectra of compounds **15**–**22**; (9) Figures S17–S18: ^{31}P NMR spectra of compounds **23a**–**b**; (10) Figure S19: ^{13}C NMR spectrum of oxetane-*A* (**1c**); (11) Figure S20: ^{13}C NMR spectrum of oxetane-*G* (**1d**). This material is available free of charge via the Internet at http://pubs.acs.org.

JA048417I

(46) Case, D. A.; Pearlman, D. A.; Caldwell, J. W.; Cheatham, T. E., III.; Wang, J., Ross, W. S.; Simmerling, C. L.; Darden, T. A.; Merz, K. M.; Stanton, R. V.; Cheng, A. L.; Vincent, J. J.; Crow-ley, M.; Tsui, V.; Gohlke, H.; Radmer, R. J.; Duan, Y.; Pitera, J.; Massova, I.; Seibel, G. L.; Singh, U. C.; Weiner, P. K.; Kollman, P. A. 2002, AMBER 7, University of California, San Francisco.
(47) Cheatham, T. E., III.; Kollman, P. A. *J. Am. Chem. Soc.* **1997**, *119*, 4805.
(48) Ausubel, F. M.; Brent, R.; Kingston, R. E.; Moore, D. D.; Seidman, J. G.; Smith, J. A.; Struhl, K. *Current Protocols in Molecular Biology*; John Wiley & Sons: New York, 1995; Vol. 3, 10.3.